SEISMIC PERFORMANCE OF FRAMED TUBE STRUCTURES

A DISSERTATION

Submitted in the partial fulfilment of the requirements for the award of the degree of

MASTER OF TECHNOLOGY

in

EARTHQUAKE ENGINEERING

(With specialization in Structural Dynamics)

by

AVANISH V

(17526005)

DEPARTMENT OF EARTHQUAKE ENGINEERING

INDIAN INSTITUTE OF TECHNOLOGY ROORKEE

ROORKEE-247 667 (INDIA)

JUNE, 2019

CANDIDATE'S DECLARATION

I hereby, declare that the work which is being presented in this dissertation report entitled, **"SEISMIC PERFORMANCE OF FRAMED TUBE STRUCTURES"**, being submitted in partial fulfilment of the requirements for the award of degree of "Master of Technology" in "Earthquake Engineering" with specialization in Structural Dynamics, to the Department of Earthquake Engineering, Indian Institute of Technology Roorkee, under the supervision of Prof. Yogendra Singh, Department of Earthquake Engineering, Indian Institute of Technology Roorkee, is an authentic record of my own work carried out during the period of June 2018 to June 2019.

I declare I have not submitted the record embodied in this report for the award of any other degree or diploma.

Place: Roorkee **Avanish V**

Date: 21 June 2019 Enrollment no. 17526005

CERTIFICATE

This is to certify that the above statement made by the candidate is correct to the best of my knowledge and belief.

Place: Roorkee **(Yogendra Singh)**

Date: Professor

Department of Earthquake Engineering

Indian Institute of Technology Roorkee

ACKNOWLEDGEMENT

I wish to express my sincere thanks and deep sense of gratitude to my supervisor **Prof. Yogendra Singh** for his valuable guidance, constant encouragement and inspiration. I am grateful for his co-operation and kind help he rendered from time to time. I feel overwhelmed for the wonderful learning opportunity and experience gained at IIT Roorkee. I am thankful to all the faculties of the Earthquake Engineering Department, IIT Roorkee for their kind help.

I would also like to thank my parents and fellow classmates for their help and moral support during the course of this work without whom this would not have been possible.

Date: 21 June 2019
Place: Roorkee

Avanish V
(17526005)

ABSTRACT

Tall buildings are subjected to high lateral loads due to wind and earthquake forces, which would lead to high costs and the design would be economically unfeasible using traditional structural systems. Hence, in order to overcome these, many structural systems have been developed, one of them is the framed tube structural system. These are efficient in withstanding lateral loads as well as economical for tall buildings. But there are a few problems with this system namely shear lag effect, which is the non-linear distribution of axial stresses in the columns causing high stresses in corner columns and low stresses in middle columns there by reducing efficiency.

In the present study, behaviour of RC framed system and its performance under gravity and lateral loads is studied using linear and nonlinear analysis. Also, the contribution of carious modes of vibration in seismic response of the building has been studied considering different number of modes.

The shear lag variation of the framed tube building is studied under different types of loading and it is found that the variation of shear lag along the height of the structure depends on the type of lateral load, relative stiffness of the beams and columns of the structure, the number of storeys and the number of bays. It is found that increasing the stiffness of the interconnecting beams significantly reduces the shear lag., mimicking the ideal tube behaviour. The shear lag behaviour is studied during nonlinear static and dynamic response as well. From the corresponding results, it is concluded that the nonlinearity in the structure did not affect the shear lag to a significant extent.

The seismic behaviour of the frame-tube structure is studied using nonlinear static and dynamic analyses. It is found that nonlinear static analysis, which considers only the fundamental mode of the structure does not depict the true behaviour of the structure. A different approach to obtain the actual behaviour of tall structure from nonlinear static analysis considering higher modes (Modal Pushover Analysis, MPA) as well is used and compared with the response obtained from nonlinear dynamic analysis. It is found that the MPA procedure gives quite accurate results for storey displacements and inter-storey drift ratios but is not suitable to obtain the plastic hinge rotations in the structure. The difference between the response of the structure obtained from the MPA and the nonlinear time history analysis is studied and it is concluded that in tall structures, the contribution of higher modes is important in assessing the seismic.

TABLE OF CONTENTS

LIST OF TABLES

LIST OF FIGURES

CHAPTER 1: INTRODUCTION

A tall building is a building which has more than 30 storeys. Such buildings usually have a symbolic and economic presence in a city. The design and construction of a tall building is different from that of conventional buildings with few storeys. With the increase in height of the building, it is subjected to higher lateral loads due to wind. Under earthquake loading, a tall building is affected differently than a regular building due to its mass and period of vibration, which largely depend on its height. Hence, the structural system of a tall building must be able to withstand these forces. In recent years, there has been a high demand for tall buildings structures because of scarcity of land, demand for housing and overall economic status of the city.

1.1 Evolution of Design of Tall Buildings

The process of designing high-rise buildings have changed over the past years. In its initial development, reinforced concrete buildings were limited to only few storeys height and the structural system used was the traditional beam-column frame system which made the construction of taller buildings relatively expensive. Then, by the introduction of shear wall system, buildings as high as up to 30 storeys were possible but taller buildings still remained economically unfeasible (Ali and Moon, 2007). Hence, to overcome these drawbacks the framed tube system was developed. The framed tube structural system has expanded in its application and in its variation over the years. One of these variations is its application with an interior shear wall known as 'Tube-in tube' system. However, each system has its own advantages and disadvantages leading to the development of newer structural systems for high rise buildings.

1.2 Objective

The objectives of this dissertation are as following:

- To assess the behaviour of a framed tube building under lateral loads including seismic forces.
- To study the variation of axial forces in the structure along the height in order to study the shear lag behaviour in framed tube buildings.
- To evaluate the performance of a framed tube building by non-linear static and dynamic analyses.

1.3 Framed tube structures

The framed tube system is a structural system which consists of closely spaced columns (usually 2-5m) along the exterior which are interconnected by deep spandrel beams, thus creating a hollow concrete tube perforated by openings for windows. This type of structural system was first apparently used on the design of the 43 storey DeWitt-Chestnut apartment building in Chicago in 1963 (Fintel, 1974).

In a Framed tube building, the main lateral load resisting systems is the perimeter beam and columns. The beam column frames in the perimeter are designed to resist the lateral loads such as Wind loads or Seismic loads. However, there can be interior columns as well but these interior columns do not provide any lateral resistance to the building. The gravity loading is shared between the exterior and the interior columns. This structural system is efficient and easy to construct and is appropriate for buildings up to 100 storeys. As shown in Figure 1.1, under the action of lateral loads, the perimeter frames along the direction of load act as the webs and those normal to the direction of load act as the flanges of a tube cantilever building.

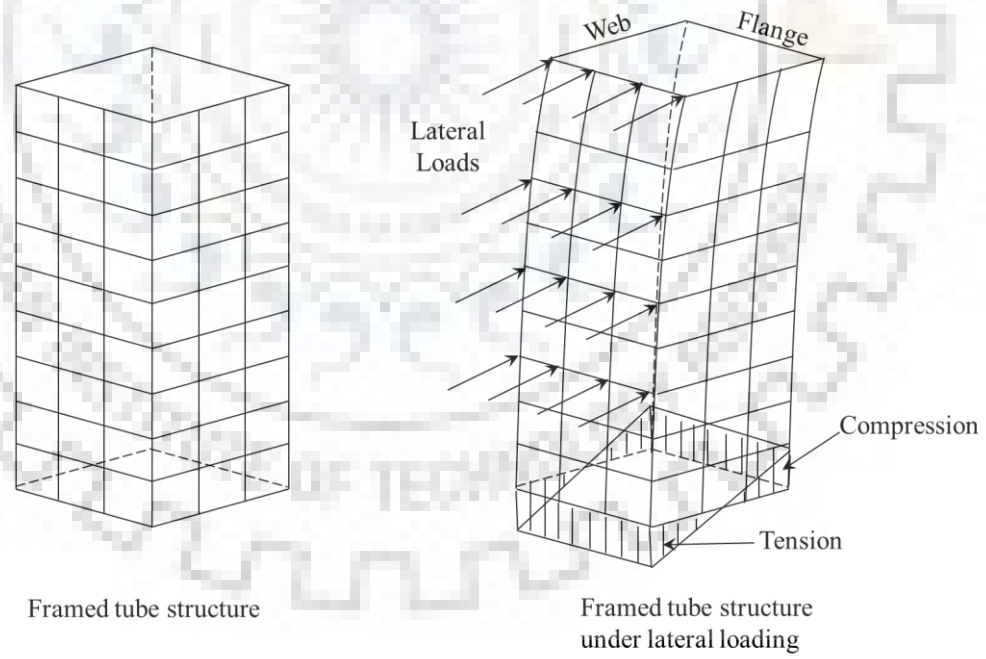

Figure 1.1 Behaviour of framed tube structures

CHAPTER 2: BEHAVIOUR OF FRAMED TUBE STRUCTURAL SYSTEM

In this dissertation, the behaviour of framed tube type of structural system under the effect of gravity and lateral loads is studied.

The behaviour of a framed tube structural system is a combination of a cantilever like shear wall and a beam column frame. The overturning moments caused by the lateral loads are resisted by the tube by tension and compression in the columns, while the shear forces are resisted by the bending in the beam column frames along the direction of the lateral load.

The framed tube system is a significant development in the construction of tall buildings since it is easy to construct and is appropriate for great heights. The only disadvantage of this system is that exact tube behaviour is not achieved due to shear lag phenomenon wherein there is an uneven distribution of axial stresses along the flange and web columns, which reduces its efficiency.

2.1 Shear Lag

The cantilever tube like behaviour of framed tube structures becomes very important, when the overturning of the structure due to lateral loads are considered. Under these conditions, the exterior column system can be considered as a rigid hollow tube. But, because of the fact that the web of the hollow tube, that is, the two sides parallel to the direction of the lateral load, are not actually solid webs, but are, in fact grid frames, there is loss of efficiency due to the flexibility of this web frame, which causes shear lag.

The main reason for shear lag is the lack of shearing of the beams in the web and flanges. If the stiffness were to be high enough (infinite), then the entire frame would behave as an ideal cantilever tube and thus there would be no effects of shear lag.

2.2 Types of Shear Lag

2.2.1 Positive Shear Lag

If the axial stresses along the flange width are high in corner columns in comparison to middle of flange, then this type of shear lag effect is called positive shear lag.

2.2.2 Negative Shear Lag

If the axial stresses along the flange width are lower in corner columns in comparison to middle of flange, then this type of shear lag effect is called negative shear lag (Figure 2.1).

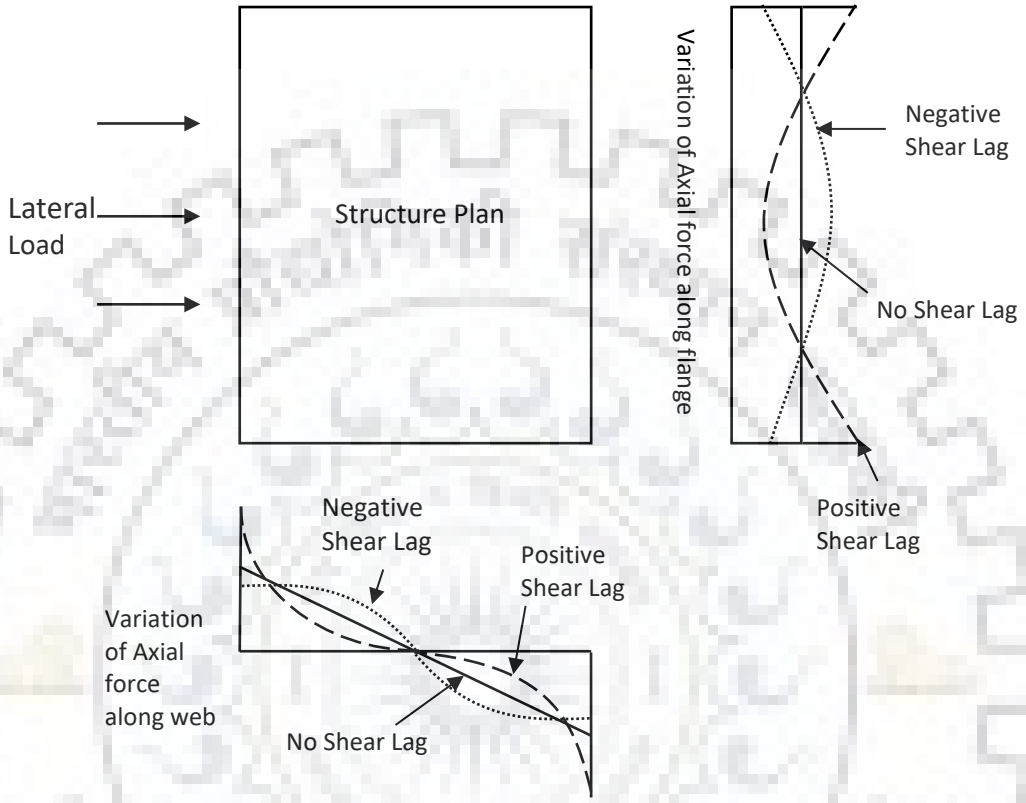

Figure 2.1 Shear lag in framed tube structures

The magnitude of shear lag effect is measured by shear lag ratio. It is the ratio of maximum stress at the corner side of the flange panel to the middle of the panel where stress is the least. This ratio quantifies the effect of shear lag in a building. A shear lag ratio of less than one indicates negative shear lag and more than one indicates positive shear lag.

Shear lag results in the perimeter columns not being evenly stressed like a tube structure and hence, the lateral stiffness reduces. Providing proper bracing at suitable heights can reduce shear lag effects. It has been found that bracing system effectively reduces shear lag effect as well as increases the lateral stiffness of the building.

2.3 Studies on Shear Lag Behaviour

Many studies have been made regarding the shear lag behaviour of frame tube structures. Singh and Nagpal (1994) investigated the variation in shear lag along the height of a framed tube structure when subjected to a lateral uniformly distributed load. A 40-storey structure was subjected to a uniformly distributed lateral load and the variation of axial force in the flange columns of the structures was studied. As in Figure 2.2, at the base of the structure, the axial forces in the corner columns is higher than in the middle columns, which is due to positive shear lag effect at the base of the structure. This shear lag decreases along the height of the structure until at a certain point where it reaches zero, after which negative shear lag occurs, represented by axial force in the middle columns being higher than, those in the corner columns.

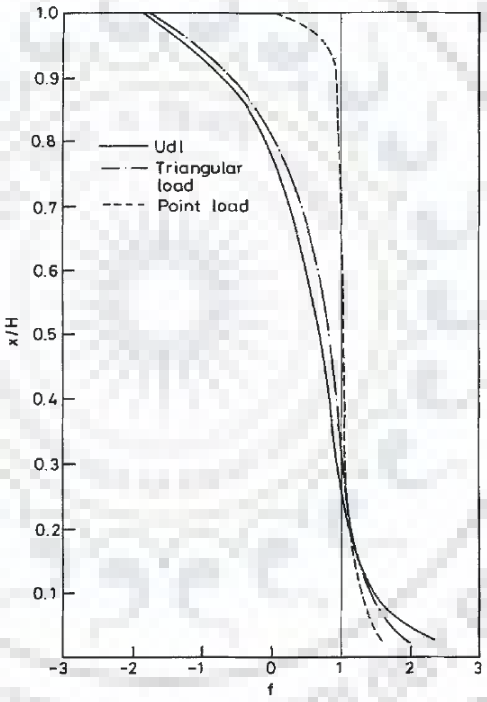

Figure 2.2 Shear lag variation in flange columns along height (Singh and Nagpal, 1994)

To explain the negative shear lag effect, they considered two modes. The first mode contributed to positive shear lag and the second mode to negative shear lag and the overall effect on the building is the combination of these two modes. They also concluded that the negative shear lag originates from positive shear lag, that is, the higher the positive shear lag, higher is the negative shear lag and the level of shear lag reversal shifts upwards. It was found that the Shear lag effect is higher for lower values of storey to span ratio and lower stiffness of the beams and columns.

Gaur and Goliya (2015) studied the shear lag effect in tall buildings with bracing system. The study included determining the best effective geometric configuration of the bracing system for reducing the shear lag effect. From their research, they have concluded that for almost all buildings of any height, the bracing angle between 45º and 63.43º is the critical variation which gives the least lateral deflection as well as shear lag ratio.

Connor and Pouangare (1991) developed a stringer-panel model for the preliminary analysis and design of a framed tube structure subjected to lateral loads. The models they developed were validated with examples and exact analysis by computer fine element software. They found that the variation of axial stresses along the height of the column depends on the relative stiffness of the beams and columns (Figure 2.3 – 2.4)

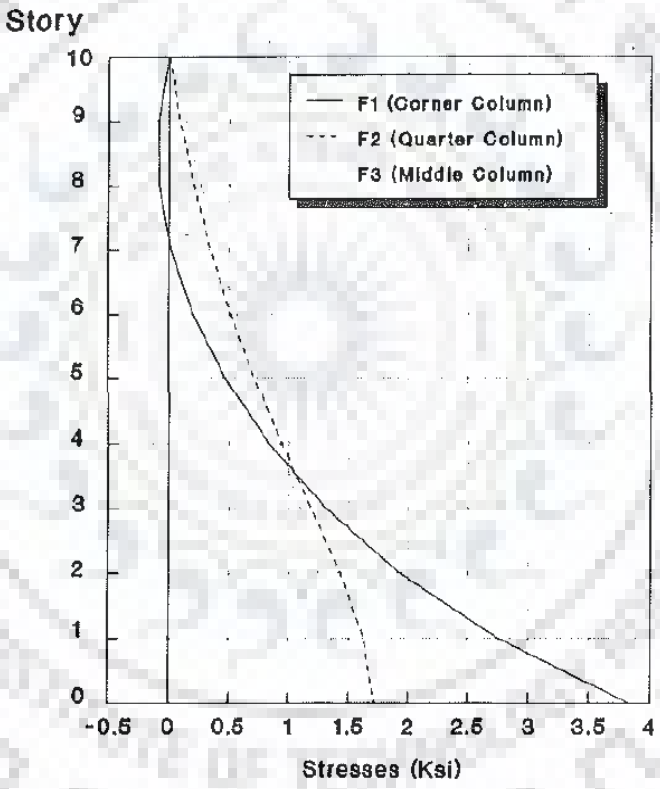

Figure 2.3 Variation of column axial stresses along height of structure with uniform properties (Connor and Pouangare, 1991)

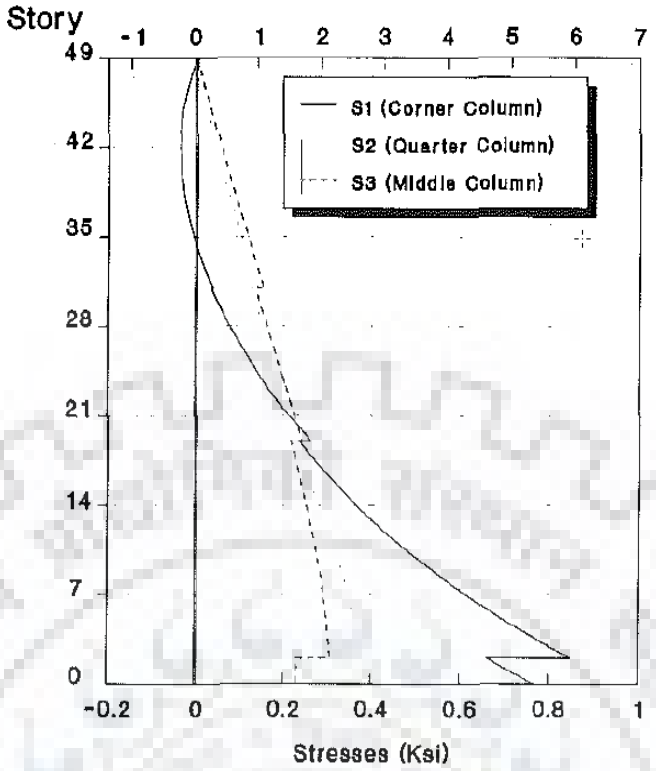

Figure 2.4 Variation of column axial stresses along height of structure with varying properties (Connor and Pouangare, 1991)

They concluded that the shear lag ratio has low dependence on the area of columns and is more dependent on the stiffness of the columns and beams. Two example structures were studied and the column axial stresses along the height was observed, one consisting of uniform and constant properties along height and the other with varying parameters.

Shinde (2017) conducted dynamic analysis of a RC framed braced tube structure under seismic loads and studied its performance. They concluded that the use of bracings effectively reduces the lateral displacement, time period of the structure and the base shear. Reduction in lateral displacement of up to 20% was achieved by using X- braced configuration.

A comparison of shear lag in tall buildings with framed tube and braced tube structures was carried out by Mazinani et al. (2014) wherein they concluded that braces along the height can actually reduce the shear lag in the building as well as control the deflection. However, apparently, the shear lag ratio does not directly affect the lateral displacement of the building, because even though braces reduced the shear lag ratio for certain configurations, the lateral displacements were quite high. Hence, an optimal

configuration needs to be chosen such that the deflection as well as the shear lag ratio is within appropriate limits.

Křístek and Bauer (1993) studied and developed a method for the determination of stress distribution in front columns of a high-rise building. They considered a model with columns and shear walls interconnected with beams and analysed the forces developed in the beams and columns when subjected to lateral uniformly distributed load. The variation of column axial forces was studied for three different cases- flexible, medium and very stiff interconnecting beams. They concluded that the stiffness of the beams has a favourable influence on the variation of stresses in the columns. However, even a very stiff beam was not able to induce a uniform distribution of the axial forces.

Shushkewich Kenneth (1991) explained the shear lag phenomenon in non-mathematical terms by considering a uniform load on a cantilever (double cantilever) as a combination of a simple beam subjected to the same uniform load and a concentrated reaction. They concluded that each component produces bending stresses with associated shear lag level. The concentrated reaction component being predominant produces positive shear lag but, the combination of the reaction component and the uniform load component causes negative shear lag near the free end. The main reason for negative shear lag is that the predominant component dampens out faster than the less predominant component.

Lee et al. (2001) explained the shear lag effect in cantilever box girder subjected to a point load. They concluded that although there is no negative shear lag when there is a point load at the free end of the cantilever, negative shear lag can be observed when the point load is at mid span. This negative shear lag beyond the mid span, in the region of zero bending moment is due to the positive shear lag in the region between the fixed end and the load. The deformation of the flange in the zero bending moment region at the point of load application to compensate the effects due to positive shear lag results in negative shear lag, also referred to as ‘Shear lag aftereffect’.

CHAPTER 3: MODELLING

In order to study the behaviour of frame tube structures under lateral loads like earthquake, a 40-storey building is modelled using the SAP2000 software. The variation of axial forces in the column is then observed and studied to have some insight into the shear lag behaviour in the structure, when subjected to lateral loads.

The behaviour of the structure is studied when the structure is subjected to different types of lateral load, namely – Uniformly distributed load, triangular load, constant acceleration, point load and earthquake loads.

3.1 Models

Two different computer models of a 40-storey building have been considered for analysis.

3.1.1 Model-1

The first model of a 40-storey building is made with uniform column and beam dimensions as 1 x 1 m. The building has plan of 27 x 27 m (Figure 3.1) with column spacing and storey height equal to 3m.

3.1.2 Model-2

The second model considered is of same plan 27 x 27 m, column spacing and storey height, but the column and beams sizes are varied along the height of the building as shown in Table 3.1.

Table 3.1 Beam and Column sizes for Model-2

Storey	**1-10**	**11-20**	**21-30**	**31-40**
Beam (B)	0.7x0.7 m	0.6x0.6 m	0.6x0.6 m	0.5x0.5 m
Column (C)	1.0x1.0 m	0.9x0.9 m	0.7x0.7 m	0.5x0.5 m

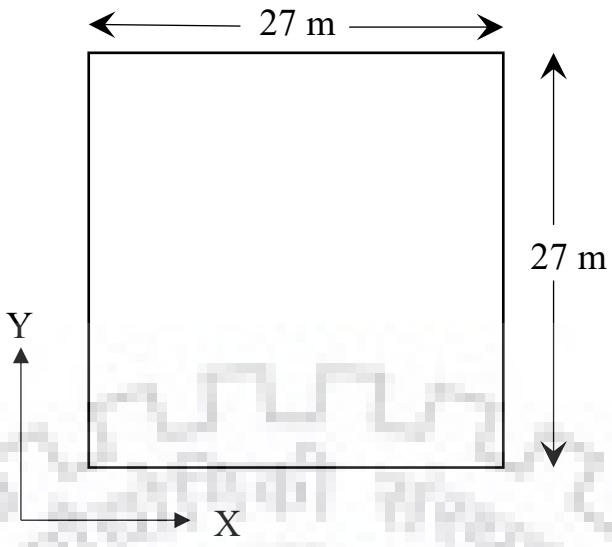

Figure 3.1 Building Plan

3.1.3 Model-3 and 4

The third and the fourth models are basically Models 1 and 2 whose beams have been made hypothetically completely rigid, that is, the shear and bending stiffness of the beams is infinite.

3.2 Damping

The damping in buildings can be of two types, namely viscous damping and hysteretic damping. The damping in a structure is usually assumed based on past studies and experimental results. Viscous damping is usually used in modelling, which gives a damping force directly proportional to the structural velocity. Based on experimental data and past studies, the typical values of damping taken are 5% for Reinforced Concrete structures and 2-3% for Steel structures. Hysteretic damping is proportional to the deformations/displacements of the structure and its elements. This type of damping takes effect, when nonlinear analysis exhibits reversal of loads or cyclic loading.

Viscous damping is modelled using Rayleigh's proportional damping and Hysteretic damping is modelled based on various types of hysteresis models predefined in SAP2000.

3.2.1 Viscous Damping

Rayleigh's proportional damping is based on mass and stiffness. It is given by

$$C = \eta M + \delta K \tag{3.1}$$

Where, η is the mass-proportional damping coefficient and

δ is the stiffness-proportional damping coefficient.

For considering model damping based on different modal frequencies, the above equation can be rewritten as

$$\xi_n = \frac{1}{2\omega_n}\eta + \frac{\omega_n}{2}\delta \tag{3.2}$$

Where, ξ_n is the critical-damping ratio and

ω_n is the natural frequency ($\omega_n = 2\pi f_n$).

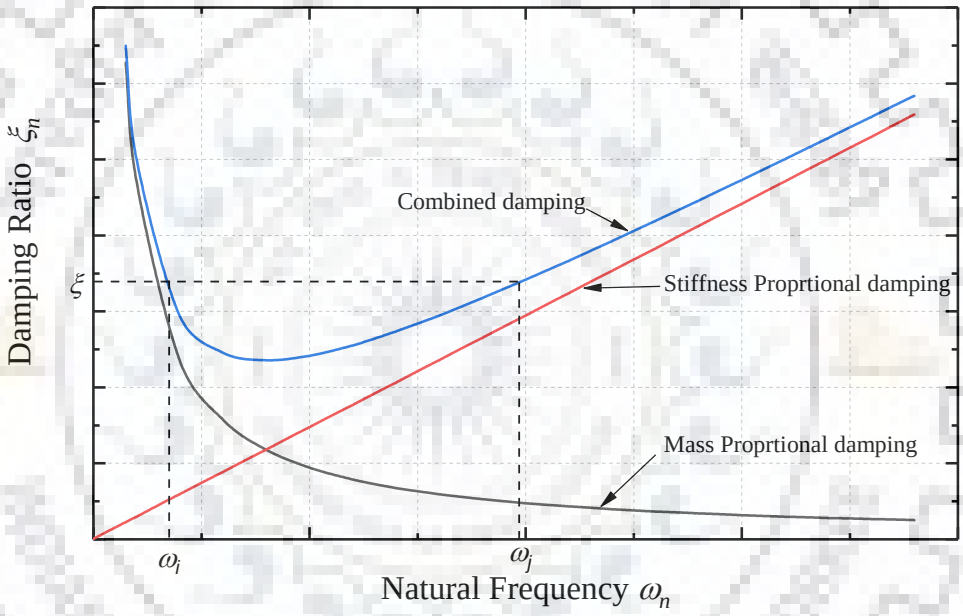

Figure 3.2 Rayleigh Damping for Constant Damping at i^{th} and j^{th} modes

The mass and stiffness proportional damping coefficients are calculated by assuming suitable damping at two different frequencies. The two frequencies/modes are selected such that 90% of modal participation is included and the corresponding damping values are based on engineering judgement, experimental data, or empirical formulae. The damping at frequencies in between are less and that outside of those frequencies are more, which can be graphically represented as in Figure 3.2.

3.2.2 Hysteretic Damping

SAP2000 provides some many hysteresis model types, namely-

- Elastic Hysteresis model

- Kinematic Hysteresis Model
- Degrading Hysteresis Model
- Takeda Hysteresis Model
- Pivot Hysteresis Model
- Concrete Hysteresis Model
- BRB Hardening Hysteresis Model
- Isotropic Hysteresis Model

Each model type is suitable for different material properties and represent different behaviour of materials. Hence, an appropriate model is to be used for appropriate elements in the model.

3.3 Assumptions

The models are made considering the following assumptions –

- The slabs are modelled as rigid diaphragms at each floor level for lateral analysis of the structure.
- The slab loads are distributed on the beams using tributary area based on yield line pattern.
- All beam-column joints are assumed rigid and modelled as rigid ends considering the beam and column sizes at that joint.
- Cracked section properties are assumed in this model. The effective stiffness values from ASCE 41-17 Table 10-5 are adopted for the beams and columns.
- The base of the structure is assumed to be fixed.
- *P-Δ* effects in the structure are considered.
- M40 grade of concrete and Fe415 grade of steel are used.

CHAPTER 4: ANALYSIS

The model is subjected to a live load of 4 kN/m^2 applied as a triangular load on the beams. A slab load of 6 kN/m^2 is also applied as a triangular load on the beams. The model is then subjected to various types of lateral loads and seismic loads.

The earthquake forces are assumed as per IS 1893-2016. Four types of analysis are carried out on these models namely –

- Linear Static Analysis (Equivalent Static Method)
- Linear Dynamic Analysis (Response spectrum Method)
- Non-linear Static Analysis (Pushover Analysis)
- Non-linear Dynamic Analysis (Time History Analysis)

4.1 Lateral Loads

The models are subjected to different types of lateral loads along the height of the building so as to study their behaviour and their effect on the shear lag in the structure.

The different types of lateral loads considered in this study are –

- A uniformly distributed lateral load;
- A triangular load with maximum intensity at the roof level;
- A constant lateral acceleration at the base of the structure; and
- A lateral point load at the roof level equal.

4.2 Static Linear Analysis

In the equivalent static analysis, the lateral force is distributed laterally on a structure proportional to its mode shape. Here, the static lateral loads substitute the effect of the dynamic effects that occur during an earthquake.

The period of the structure for the first mode is obtained from modal analysis and corresponding value of spectral acceleration (Sa/g) is calculated from IS 1893 – 2016 for soft soil site. The structure is assumed to be in Zone V (Z=0.36), the importance factor (I) is taken as 1 and a response reduction factor (R) of 5. If W is the seismic weight of the structure, then the design horizontal seismic coefficient A_h and the design lateral force is given as follows –

$$A_h = \frac{Z}{2}\frac{S_a}{g}\frac{I}{R} \tag{4.1}$$

$$V_B = A_h W \tag{4.2}$$

This static base shear is compared with the base shear obtained by using response spectrum method for the design of columns and beams.

4.3 Response Spectrum Method

This is a dynamic linear method which takes the contribution of other natural modes of vibration of the structure also into account and gives the maximum response of the building. The response spectrum method is more accurate than the static method. As per IS code provisions, the number of modes to be considered along each direction should be such that at least 90% modal mass participation is achieved and if the base shear calculated (V_B) is less than the static base shear ($\overline{V_B}$), the force response quantities must be multiplied by $\frac{V_B}{\overline{V_B}}$.

For design purposes, response spectrum analysis is performed considering *P-Δ* effects along both the directions in horizontal plane and the vertical direction as well. The design force considered is the directional combination of the forces by SRSS.

As per IS 16700 – 2017, the minimum design base shear coefficient shall not be less than 0.024 for seismic zone V. Hence, appropriate scale factors are used to increase the obtained base shear value.

4.4 Pushover Analysis

Pushover analysis gives an approximate behaviour of a structure when subjected to lateral loads. The capacity of the building can be estimated from pushover analysis.

In pushover analysis, the building is pushed in the lateral direction gradually with increasing magnitude until a desired lateral displacement is achieved. Pushover analysis is a nonlinear static analysis procedure which is performed after the application of gravity loads, that is, the stiffness at the end of the gravity load case is used as the initial stiffness for pushover analysis.

For this analysis, SAP2000 finite element software has been used. The forces are applied on the building proportional to its first mode shape and continued till the target

displacement is reached or the failure of the building. The failure point is determined when the building has developed sufficient number of plastic hinges to form a mechanism or the structure becomes unstable due to formation of hinges in all the columns of a storey which results in convergence errors and the program stops.

For Pushover analysis, hinges are assigned as per ASCE 41-17. P-M2-M3 hinges for columns and M3 hinges for beams. The hinges assigned need to been validated by comparing the hinge values with that obtained by SAP section designer and SP -16 of IS 456 – 2000.

4.5 Modal Pushover Analysis

The Pushover analysis normally carried out gives the behaviour of the structure corresponding to its first mode only. This is a pretty good estimate for a building whose modal mass participation in the first mode is high (>90%) but, for buildings whose modal mass participation in the first mode is not enough, the pushover analysis is not an accurate method.

However, since the present model is a 40-storey building, the contributions of other higher modes also need to be considered. Hence, a new approach to pushover analysis has been introduced which includes the contribution of higher modes called the Modal Pushover Analysis. A Modal Pushover Analysis needs to be performed which would give a more accurate assessment of the structures' capacity.

Chopra and Goel (2002) have suggested the Modal Pushover Analysis procedure to estimate seismic demands. The results obtained by this procedure were compared with results from an exact (Non-linear time history) analysis for accuracy.

They performed the MPA procedure for a 9-storey building and compared it with the 'exact' results, which is by nonlinear response history analysis (RHA). They found that the MPA gives a more accurate appropriate behaviour of structure in comparison with Nonlinear Response history analysis. The contribution of the second mode resulted in significant improvement in the results namely lateral displacements and storey drift. However, they found that the contribution of the third mode was quite negligible (Figure 4.1).

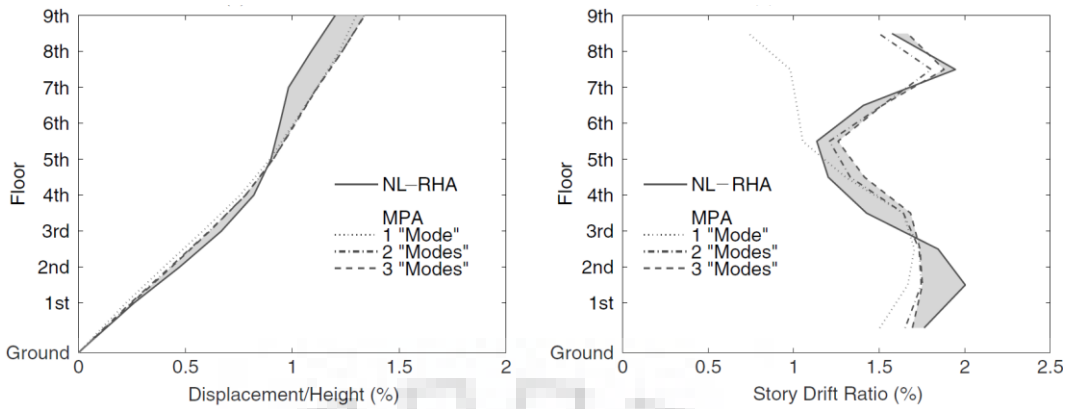

Figure 4.1 Lateral Storey displacements and storey drift ratios from MPA and non-linear RHA for 1.5×El Centro ground motion; shading indicates errors in MPA including three 'modes' (Chopra and Goel, 2002)

It was concluded that for the 9-storey building they considered, the MPA underestimates the displacements of the lower storeys and overestimates the displacements of the upper storeys. The drifts were underestimated in the lower storeys, overestimated in the middle storeys and slightly varied about the exact values in the upper storeys. But, the errors in plastic hinge rotations determined by MPA using 3 modes were very large. Hence, in the present study, plastic hinge rotation will not be calculated or studied by MPA.

The steps followed in this procedure are as follows:

- The natural frequencies, ω_n and modes, Φ_n for elastic vibrations of the structure is calculated. The number of modes required should be sufficient so as to achieve at least 90% modal mass participation.
- For each of the 'n' modes, the base shear-roof displacement, $V_{bn} - u_{rn}$, pushover curve is developed by a non-linear static analysis of the buildings as explained above (Pushover Analysis).
- The pushover curves obtained for each of the different modes are then idealized and converted into a set of capacity curves of the corresponding SDOF system using Acceleration Displacement response spectrum conversion methods. In this study, ATC-40 guidelines have been followed to obtain the capacity spectrum.
- Now, the peak deformation D_n of the 'n'th mode of each SDOF system is computed either by a non-linear response history analysis or by inelastic design spectrum.

- The peak roof displacement u_{rn} for each pushover curve corresponding to each of the 'n' modes are calculated from $u_{rn} = \Gamma_n \Phi_n D_n$.

  Where, Γ_n – the modal mass participation of 'n'th mode

- The desired responses (Inter-storey drift, Plastic hinge Rotations etc.) can now be extracted from the pushover database at roof displacement equal to u_{rn} independently for each mode. These responses in the 'n' modes are combined using SRSS to obtain a combined peak response.

4.6 Time History Analysis

Time history analysis is a step-by-step analysis of the dynamic response of a structure to a specified loading (earthquake) that varies with time. Time history analysis is used to obtain a more accurate seismic response of the structure under dynamic loading of a representative earthquake. In this type of analysis, the response of the structure at each time step specified can be obtained, which aids in properly studying the behaviour of the structure. Another advantage of time history analysis is the ground motions/loading can be applied in multiple directions simultaneously. Time-history analysis can be carried out for linear or nonlinear evaluation of dynamic structural response under loading.

4.6.1 Linear Time History Analysis

Linear time history analysis was first performed to get an idea of the behaviour of the structure when subjected to the earthquake. The performance of the building in the linear range can be compared to the results obtained from other linear analysis like that of response spectrum and equivalent static analysis. Although linear time history analysis does not include the nonlinear behaviour of the structure, it will give some insight when compared with the corresponding non-linear analysis.

4.6.2 Non-linear Time History Analysis

Non-linear time history analysis is considered the most reliable and accurate assessment of a structure under earthquake loading. But it is not preferred because of high computational time and effort required to perform the analysis. In non-linear time history analysis, the non-linearity is introduced in the structure by assigning hinges at locations. These hinges represent the non-linearity of the specific elements. In time history analysis, the loading directions is reversed/keeps changing with time, repeated cycles of loading and unloading, hence these hinges must represent the hysteresis behaviours of the

elements as well. The hinges, their properties and hysteresis parameters will be explained in detail in following chapters.

4.7 Ground Motions

ASCE/SEI 7-16 guidelines are followed for the selection of ground motions. As per the code, a suite of 11 ground motions need to be selected for the target spectrum along both orthogonal directions. The vertical seismic ground motions are not considered in this study because there are no vertical irregularities in the structure and hence, the effect of the vertical seismic forces is negligible. The ground motions selected are to be scaled either by amplitude scaling method or by spectral matching for a particular period range of the structure under consideration. This period range has an upper bound greater than or equal to 2 times the largest first-mode period and a lower bound equal to the period at which at least 90% mass participation is achieved. The ground motions selected are then applied at the supports of the structural model.

CHAPTER 5: RESULTS AND DISCUSSIONS

5.1 Gravity Loads

The total dead loads include the self-weight of the columns and beams and the slab load which has been applied as an equivalent triangular load.

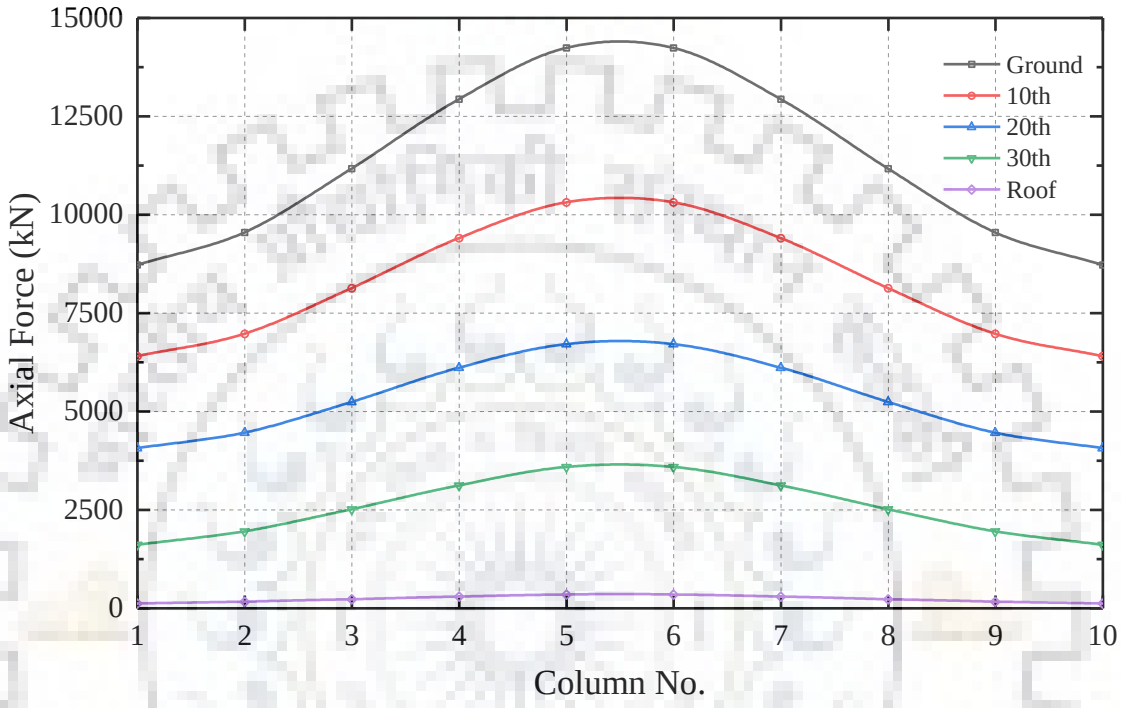

Figure 5.1 Variation of axial force in the columns under gravity loads

The variation of axial force under gravity loads is same in both the models, with higher axial force in the central columns than the corner columns as shown in Figure 5.1. This is due to the triangular/trapezoidal variation of the slab loads on the beams. As the storey height increases, the gravity loads also consequently decreases and is the least at the roof/top storey.

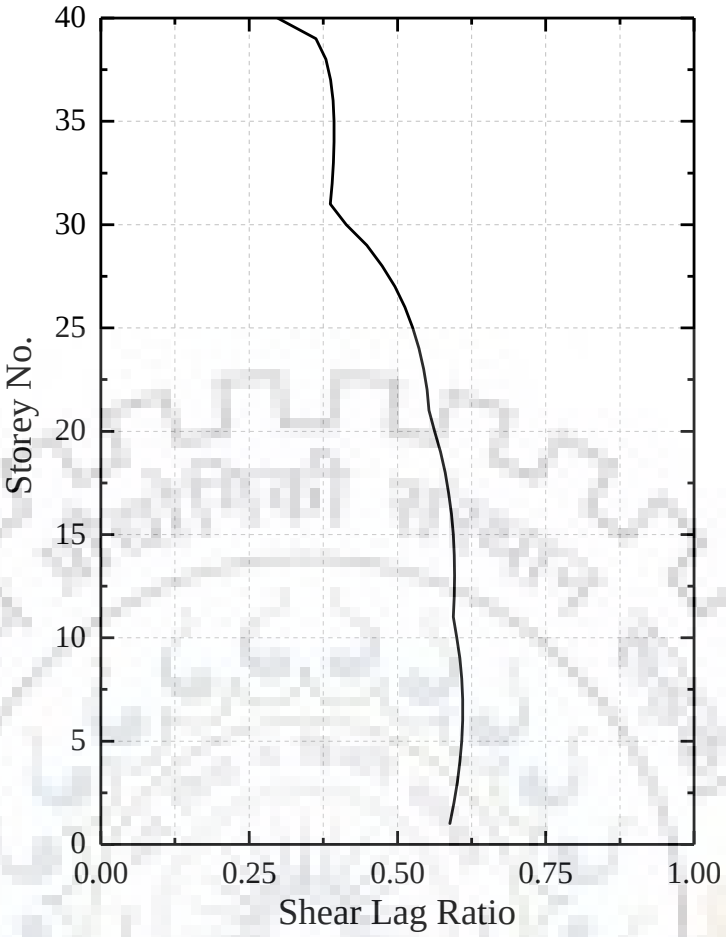

Figure 5.2 Shear lag Ratio under gravity loads in Model-2

Figure 5.2 shoes the variation of shear lag along the height under gravity loads. It can be observed that the axial forces in the middle columns are higher than the axial forces in the corner columns until the 30th storey, after which the shear lag ratio decreases to almost half. This is due to the change in the relative stiffness of the beams and columns, which decreases after every 10 storeys along the height.

5.2 Modal Analysis

Modal analysis was carried out on the structure to obtain the frequencies and mode-shapes of the building and their corresponding modal mass participation.

As can be seen from Table 5.1, a mass participation of 90% is achieved after inclusion of 10 modes. For buildings of lower height (low to mid-rise structures), the modal mass participation in the first mode itself is quite high, whereas in tall buildings that is not the case and hence, the effects of higher modes need to incorporated in all analysis.

Table 5.1 Modal Mass Participation

Mode	Period(s)	Mass Participation X	Mass Participation Y	Sum modal mass participation in X	Sum modal mass participation in Y
1	4.69	0.65	0.00	0.65	0.00
2	4.69	0.00	0.65	0.65	0.65
3	3.33	0.00	0.00	0.65	0.65
4	1.94	0.15	0.00	0.79	0.65
5	1.94	0.00	0.15	0.79	0.79
6	1.45	0.00	0.00	0.79	0.79
7	1.13	0.00	0.08	0.80	0.87
8	1.13	0.08	0.00	0.87	0.87
9	0.87	0.00	0.00	0.87	0.87
10	0.78	0.03	0.01	0.90	0.90

A modal participation factor of up to 90 % in vertical direction is obtained after 150 modes. Hence, for all future analyses, up to 150 modes have been taken into consideration.

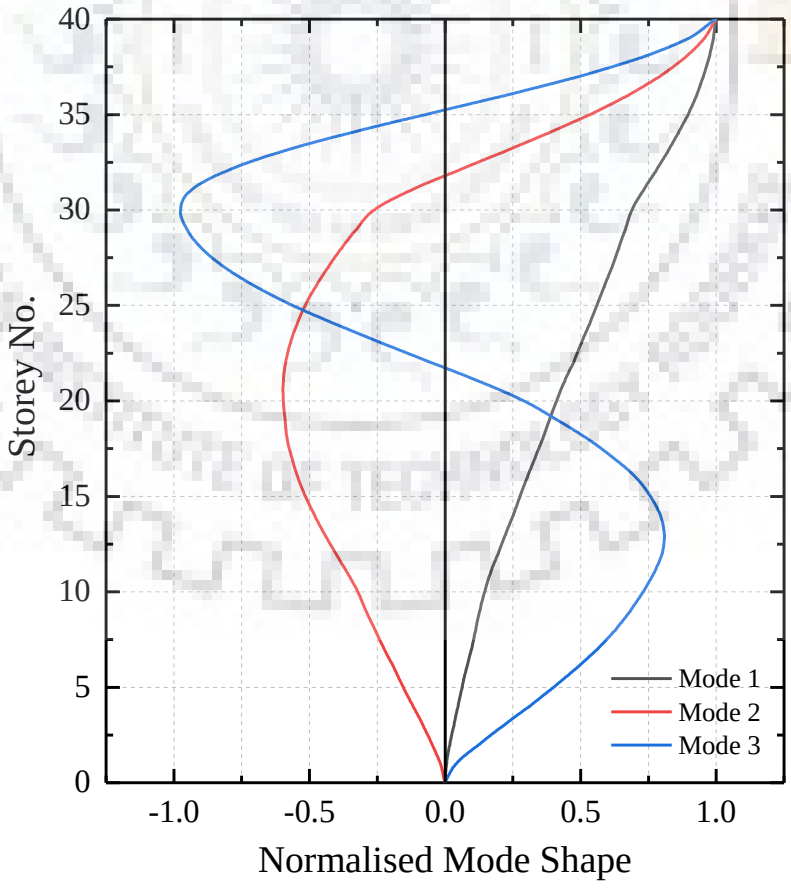

Figure 5.3 First three translational Mode shapes

Since the structure is symmetric (Figure 3.1), the frequencies and mode shapes are same in both the directions and hence the first three modes (normalised by the maximum ordinate) in one direction have been shown in Figure 5.3, and will be used in future analyses as well. Since the building is symmetric, its centre of mass and rigidity coincide, hence the effect of torsional mode will be ignored since it is a torsional stiff building.

5.3 Shear Lag under Lateral loads

The results obtained from all the above mentioned analyses were observed and studied for shear lag behaviour. In the current study, the shear lag variation along the flange of the building only is studied. The axial forces along the height of corner and middle columns have been plotted as shown in Figure 5.4.

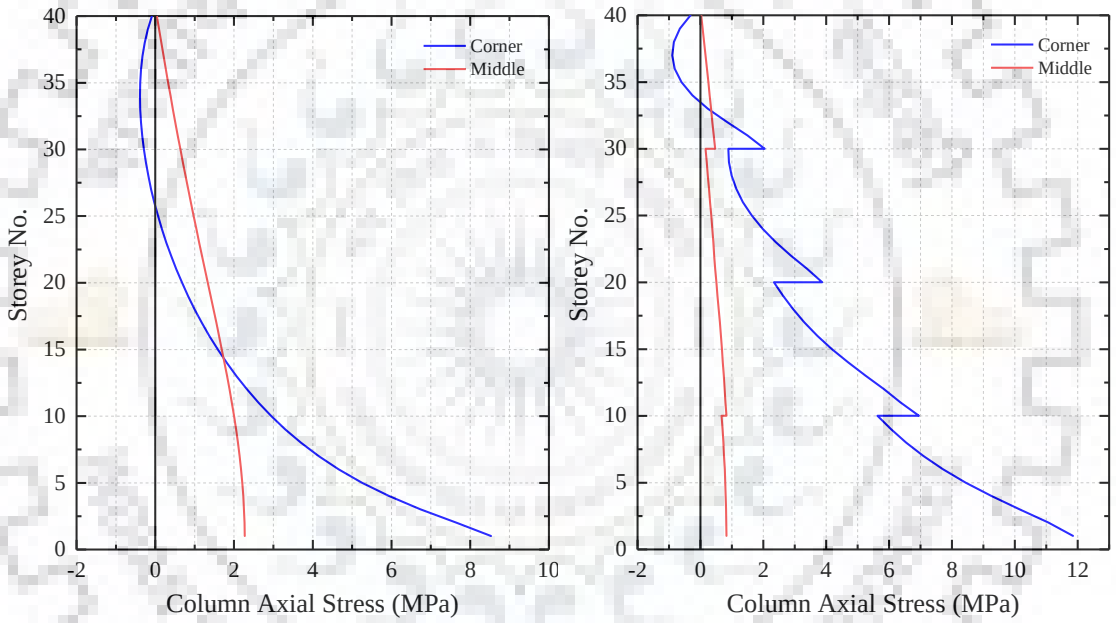

Figure 5.4 Variation of axial stress in the flange of the considered frame tube buildings, along the height, when subjected to lateral UDL in: (a) Model-1 and (b) Model-2

The axial stress variation in the corner and middle columns along the height for Model-1 is smooth because of uniform structural properties along the height and that for Model-2 shows stepped changes at regular intervals, as obtained by Connor and Pouangare (1991). This is due to the change in column and beam sizes and hence stiffness at the storeys along the height.

The shear lag behaviour is measured using a non-dimensional parameter called ‘Shear Lag Ratio’, given as ratio of the axial stresses in the corner column to the middle column.

Further, a Shear Lag ratio of 1 would mean no shear lag and values less than and greater than 1 indicates 'Negative' and 'Positive' shear lag respectively.

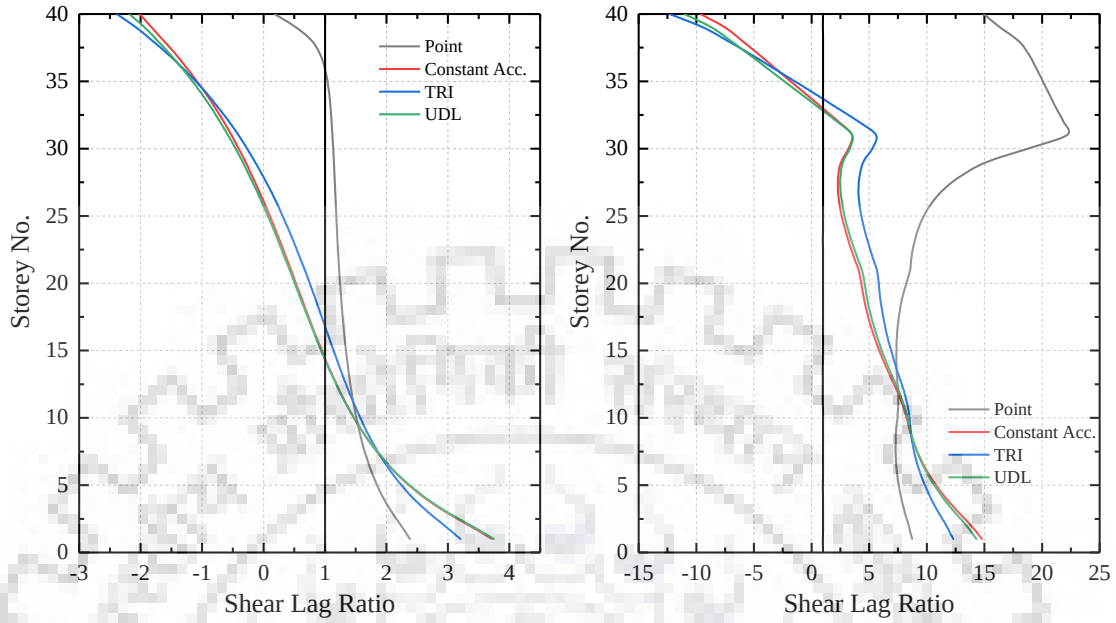

Figure 5.5 Variation of Shear lag ratio in the flange of the considered frame tube buildings, along the height, when subjected to lateral loads in: (a) Model-1 and (b) Model-2

The Shear lag variation in Figure 5.5 along the height for Model-1 shows that the shear lag reversal takes place at around the 15th storey for UDL, at the 17th storey for lateral triangular load and near the upper storeys for point load. A similar variation was observed by Singh and Nagpal (1994) for the same type of loads, the slight upwards shift in shear lag reversal here compared to their study is due to higher number of bays considered which results in higher shear lag and upward shift of its reversal in the structure. This validates the current model taken and further cements this behaviour in framed tube structures.

The shear lag reversal for Model-2 occurs at around the 33rd storey for all the lateral loads except the point load. For the point load, it is observed that shear lag reversal does not take place, that is, there is no occurrence of negative shear lag. The properties of the beams and columns in Model-2 vary along the height and is not constant as in case of Model-1. Hence, the shear lag reversal has shifted upwards. However, the actual positive and negative shear lag magnitude has increased by about 5 times, owing to the reduced lateral stiffness of the building.

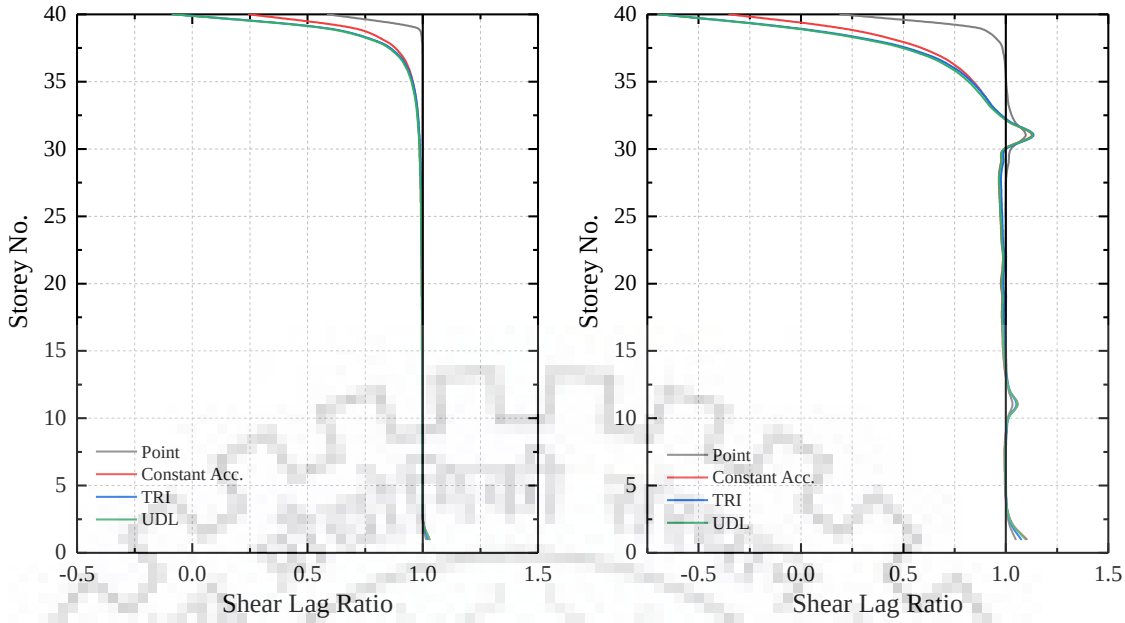

Figure 5.6 Variation of Shear lag ratio in the flange of the considered framed tube buildings, along the height, when subjected to lateral loads in: (a) Model-3 and (b) Model-4

From Figure 5.6, it is clear that increasing the beam stiffness to make it rigid has had a huge influence on the shear lag. The shear lag in both Model-3 and Model-4 has been almost completely eliminated. Although, the shear lag has reduced significantly, negative shear lag can be seen in the upper storeys in both the Models, which is due to finite stiffness of beams and is negligible.

5.4 Equivalent Static Method

The fundamental periods of the two models were obtained by modal analysis. Based on the period, the respective values of seismic coefficients were obtained as per IS 1893-2016 to calculate the base shear on the structure (Table 5.2).

Table 5.2 Static Base Shear

Model No	**1**		**2**	
Time Period (s)	3.031		4.685	
Seismic Weight (kN)	W = 449216.22		W = 341634.68	
Design Seismic Coefficients	A_h= 0.0198	A_v = 0.06	A_h= 0.015	A_v = 0.06
Design Base Shear (kN)	$V_{x,y}$= 8910.22	V_z=26952.97	$V_{x,y}$= 5112.73	V_z=20498.08

5.5 Response Spectrum Method

Response spectrum analysis is performed on the structure taking into account first 150 modes of vibration so as to achieve 90% modal mass participation along all three directions (Two horizontal and one vertical).

Table 5.3 Response Spectrum Method

Model No.	**1**		**2**	
Seismic Coefficient	A_h = 0.0176	A_v=0.049	A_h = 0.0135	A_v=0.04
Base shear (kN)	$V_{x,y}$= 7926.38	V_z = 22177.89	$V_{x,y}$= 4274.68	V_z = 13799.83

The design seismic coefficient obtained (Table 5.3) as per analysis is less than the minimum basic seismic coefficient specified in IS 16700-2017. Hence, suitable scale factor has been used to obtain the design base shear which have been tabulated in Table 5.4. The design force considered is a directional combination of the base shear in both directions by SRSS rule. Since the building is symmetric, the base shear as well as variation of the forces is same along both the directions.

The variation of shear lag ratio in the flange columns along the height of the two models have been plotted to observe their behaviour along the height of the building.

Table 5.4 Response Spectrum Method Design base shear

Model No.	**1**		**2**	
Basic Seismic Coefficient	A_h = 0.024	A_v=0.06	A_h = 0.024	A_v=0.07
Design Base shear (kN)	$V_{x,y}$=10836.43	V_z = 27145.74	$V_{x,y}$ =8198.85	V_z = 26468.03

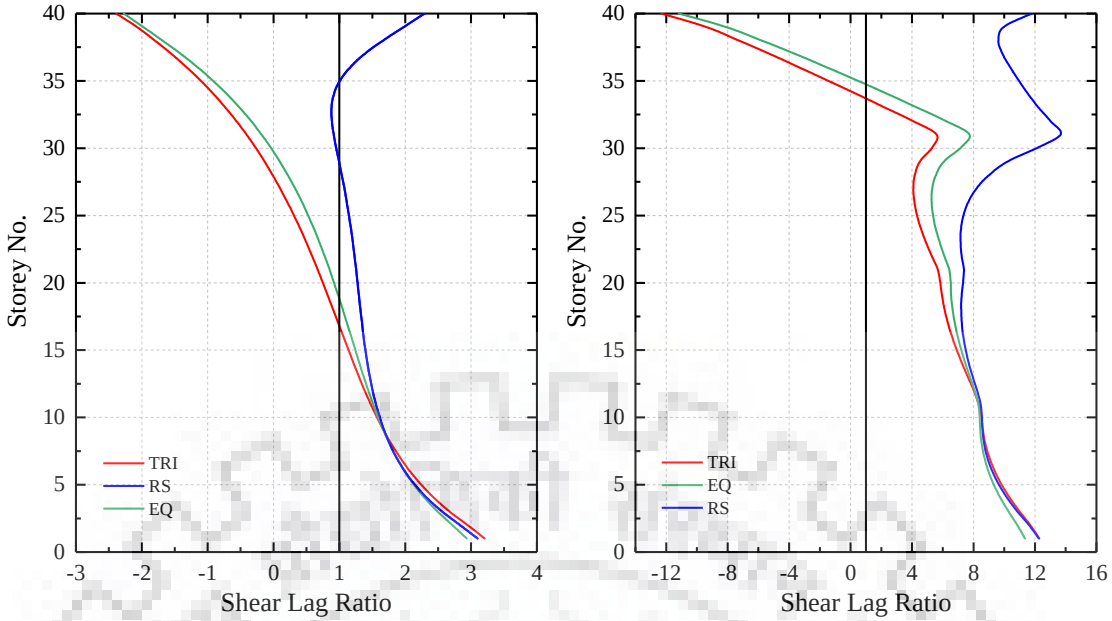

Figure 5.7 Variation of Shear lag ratio in the flange of the considered framed tube buildings, along the height, when subjected to equivalent static and response spectrum loading in: (a) Model-1 and (b) Model-2

From Figure 5.7, it can be observed that the shear lag variation under equivalent static load is similar to the variation under lateral triangular load. This is reasonable because, the lateral loads are applied as per IS 1893-2016. As per code, the loads are applied based on the first mode shape of the building and the mode shape is assumed to be directly proportional to h^2, where h is the height from the bottom to the storey considered. This parabolic variation of lateral load along height is quite similar to the triangular variation. The shear lag at the bottom storeys is slightly reduced but, at higher storeys it starts increasing gradually. The shear lag ratio under response spectrum loading has a different variation than that of equivalent lateral loading, this is due to the modal combination of forces by SRSS, which yields a positive result ignoring the change in sign of the forces.

5.6 Design

The structure needs to be designed for forces obtained from above analysis. The beams and columns after static and response spectrum analysis are designed for load combinations including earthquake loads as per IS 1893-2016 and IS 456-2000. The design of the building is also governed by the guidelines present in IS 16700-2017, which suggests the following-

- Spacing between columns must not be more than 5m.

- Avoid re-entrant corners and sharp changes to tubular form.
- Corner columns shall be at least 1-2 times that of internal column.
- Height to width ratio of openings shall be similar to ratio of storey height to column spacing.
- Due consideration to be given to shear lag effects in design.
- The value of inter-storey drift stability coefficient should not exceed 0.20.

5.6.1 Design Load Combinations

The design load combination of forces for which the structure is designed for as per IS 1893-2016 is as follows:

Combination 1 - $1.2\ (DL + IL \pm EL)$ (5.1)

Combination 2 - $1.5\ (DL \pm EL)$ (5.2)

Combination 3 - $0.9\ DL \pm 1.5\ EL$ (5.3)

Where, DL - Dead Load

IL - Imposed Live Load

EL – $\sqrt{(EL_x)^2+(EL_y)^2+(EL_z)^2}$ Earthquake Load

The reinforcement provided after analysis considering the all the load combinations mentioned in Equations (5.1-5.3) have been tabulated in Table 5 5.

Table 5.5 Column and Beam reinforcement

Storey	**1-10**	**11-20**	**21-30**	**31-40**
Column Size	1.0 x 1.0 m	0.9 x 0.9 m	0.7 x 0.7 m	0.5 x 0.5 m
Reinforcement	2.71%	2.736%	2.01%	2.955%
Beam Size	0.7 x 0.7 m	0.6 x 0.6 m	0.6 x 0.6 m	0.5 x 0.5 m
Reinforcement	1.32%	2.075%	1.855%	2.2%

5.6.2 Torsion Irregularity

As per IS 1893-2016, the following two torsional irregularity checks have been suggested-

a. The maximum horizontal displacement of any storey in the direction of lateral force at one end should not be more than 1.5 times its minimum horizontal displacement at the other end of the same floor in that direction.

b. The natural period of the fundamental translational modes in each direction should be more than the natural period of the fundamental torsional mode.

The ratio of displacement of a storey at one end to that in the other end have been checked taking minimum eccentricity as per code equal to 5% of the plan dimension perpendicular to direction of force and found to be within permissible limits (Table 5.6).

Table 5.6 Torsional Irregularity check

Storey No.	Delta max (mm)	Delta Min (mm)	Ratio
1	0.933	0.841	1.109
10	20.356	18.716	1.087
20	56.368	51.988	1.085
30	94.519	87.333	1.082
40	137.432	127.044	1.081

The natural period of the fundamental torsional mode was found to be 3.325s and is less than that of the first two translational modes which are 4.685s along both directions.

The code also specifies design for torsion as well, wherein the shear forces in the lateral force resisting system is increased. This increase in forces is however, based on the distance between the centre of mass and rigidity, which in the current case is zero due to symmetry and accidental torsion. Hence, the increase in forces only due to accidental torsion has been considered in the design.

5.6.3 Stability Coefficient

The stability Coefficient θ considers the effect of the P-Δ effect in building. As per IS 16700-2017, it should be less than 0.2. However, range and its use in design has not been clearly specified in the code. Hence, Euro code EC-8 is referred to as it also defines a stability coefficient of the same formulation. It is given by,

$$\theta = \frac{P_u \Delta}{V_u H} \tag{5.4}$$

where P_u is the design storey vertical load, V_u the design storey shear, Δ the design inter-storey drift and H the inter-storey height.

As per EC-8, the limit is 0.1 and if the coefficient is in between 0.1 and 0.2, suitable amplification factor α has to be applied to the displacements and internal forces given by Equation (5.5). However, a stability coefficient of more than 0.2 is considered unacceptable.

$$\alpha = \frac{1}{1-\theta} \tag{5.5}$$

De Stefano et al. (2004) found that stability coefficient less than 0.1 also cannot be neglected based on their study of probabilistic evaluation of second order effects in RC structures subjected to earthquakes. They found that P-Δ effects can significantly increase inelastic deformations if not considered properly in design of the structures.

Table 5.7 Stability Coefficient of storeys

Storey No.	**Design Storey Shear V_u (kN)**	**Inter-storey drift Δ (mm)**	**Design Gravity load P_u (kN)**	***H* (m)**	**θ (rad)**
1	8767.87	3.07	244400.00	3.00	0.03
10	11139.73	6.72	182019.50	3.00	0.04
20	8863.86	9.06	123744.78	3.00	0.04
30	4540.30	8.32	51457.69	3.00	0.03
40	1258.50	6.50	5200.07	3.00	0.01

In the current study, IS code is being followed, hence, the stability coefficients have been checked and are found to be well within the limits (Table 5.7).

5.7 Pushover Analysis

Model-2 represents the realistic design as column and beam dimensions are varied along the height of the building. Hence, the pushover analysis of Model-2 only has been performed and its behaviour studied.

5.7.1 Plastic hinges

The beam and column sizes obtained after design and further used in pushover analysis have been tabulated in Table 5.5. The plastic hinges are then auto assigned to beams and columns as per ASCE 41-13 in SAP2000, taking expected strengths of concrete and steel into account. The beams are assigned M3 moment only hinges as it is expected to form hinges in bending and the columns are assigned P-M2-M3 hinges. The plastic hinge position has been taken $L_p/2$ from the face of the column or beam, where L_p is the plastic

hinge length, given by L_p=0.5H (Park and Paulay, 1975), where H is the depth of the section.

This formulation to calculate hinge location has been found to be sufficiently accurate and the hinges auto assigned by SAP2000 is reasonable accurate if the corresponding hinge properties have been properly checked and verified and only if the building has not been designed by pre-modern codes (Inel and Ozmen, 2006).

Expected strength of concrete = 1.5f_c' = 48 MPa

Expected strength of steel = 1.25f_y = 518.75 MPa

The moment hinge assigned to beams considering their yield moment and rotations as per ASCE 41-17 is as shown in Figure 5.8, where the yield moment has been computed through the frame *P-M* interaction.

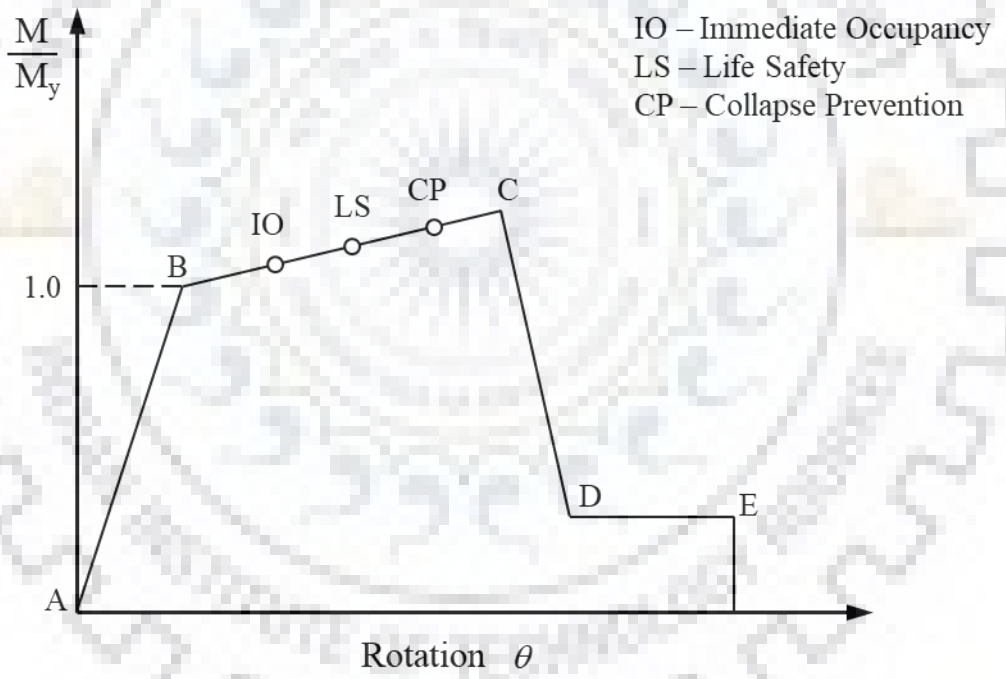

Figure 5.8 Back-bone curve for beam moment hinge as per ASCE 41-17

Similarly, the column P-M2-M3 hinge properties considered is compared with IS code P-M2-M3 interaction surface. Since the columns are square sections, the capacity in both the directions are same and hence, P-M2 interaction only is compared as shown in Figure 5.9.

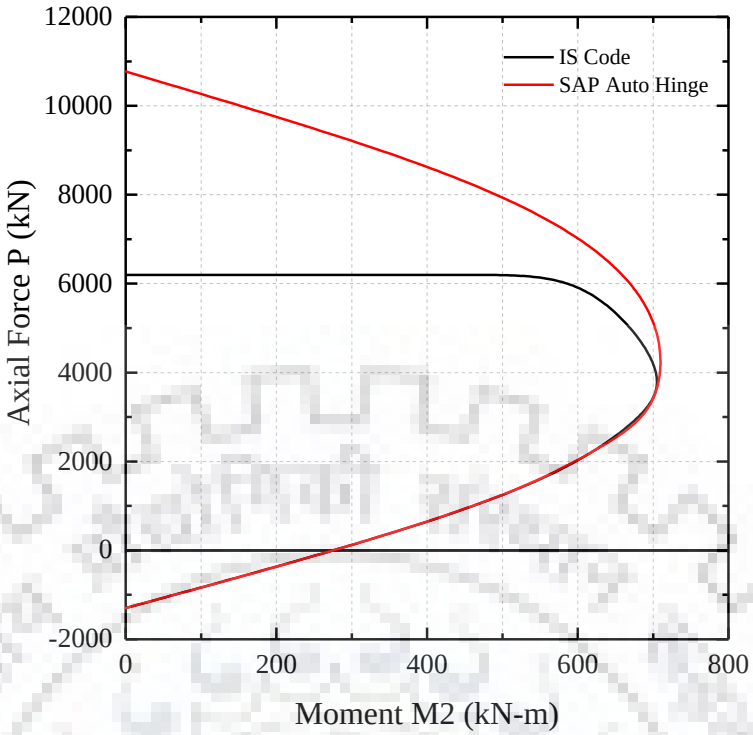

Figure 5.9 P-M2 interaction surface comparison of the hinge and IS code

From Figure 5.9, it can be seen that P-M2 values of the hinge is in close correlation with that of IS code after the initial few values. This is because, the initial maximum value of axial force is defined in IS 456-2000 for short axially loaded members in compression considering minimum eccentricity given by Equation (5.6).

$$P_u = 0.4 f_{ck}.A_c + 0.67 f_y.A_{sc} \quad (5.6)$$

Where, P_u is the axial load capacity, A_c is the area of the concrete section, A_{sc} is the area of steel, f_{ck} is the expected compressive strength of concrete and f_y is the yield strength of steel.

For comparison with hinge properties, the corresponding expected strength values have been assumed for steel and concrete in Equation (5.6).

5.8 Modal Pushover Analysis

The modal mass participation factor of the model in the first fundamental mode along X-direction is 65%. Hence, a pushover analysis considering only one mode will not give the realistic behaviour of the structure. Hence, modal pushover analysis has to be performed.

In the current model, a modal mass participation of 90% is achieved by considering 10 modes. Hence, the pushover analysis is performed using loading patterns as per the 10 modes. Since, the building is symmetric in plans and elevation, the pushover analysis is considered only in one plane, that is, the first three modes along one direction only are considered.

5.8.1 Mode 1 Pushover analysis

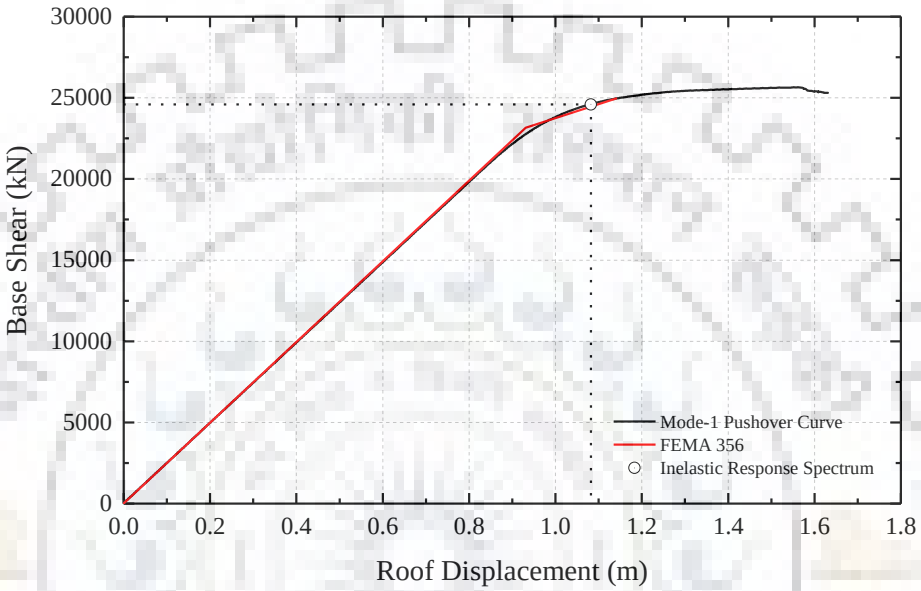

Figure 5.10 Mode 1 Pushover curve

The pushover curve obtained from analysis shown in Figure 5.10 is bi-linearized using FEMA 365-2000 guidelines. After equivalent bi-linearization of the curve, the over strength factor and ductility capacity of the building have been calculated and tabulated in Table 5.8.

The Peak deformation of the 1st mode inelastic SDOF system from the inelastic response spectrum has been marked on the graph, determined by ATC-40 guidelines which will be used later for modal combination.

Table 5.8 Pushover analysis results

Design Base shear (V_d)	8198.85 kN		
Base shear at yield (V_y)	23456.24 kN	**Yield displacement (Δ_y)**	0.91 m
Base shear at failure	25306.53 kN	**Maximum displacement (Δ_{max})**	1.63 m
Overstrength Factor (V_y/V_d)	2.86	**Displacement ductility ratio (μ)**	1.79

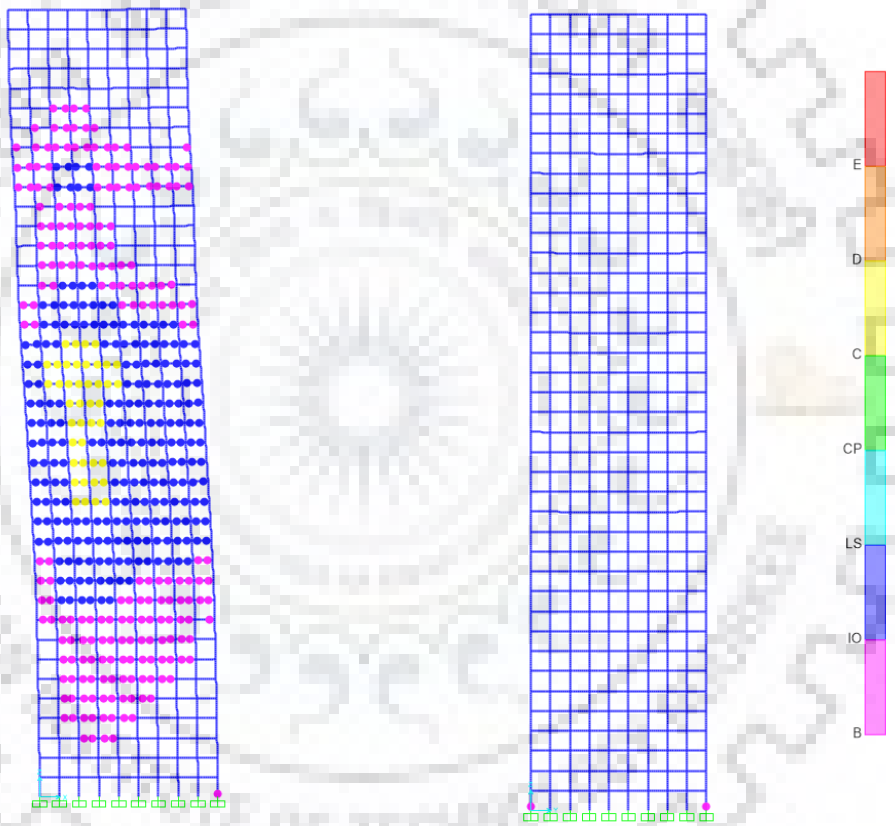

(a) (b)

Figure 5.11 Formation of hinges at the end of pushover analysis along Mode-1 in (a) X-Z plane (Web) and (b) Y-Z plane (Flange)

From the pushover analysis, it is observed that the first hinges form in beams at the 22nd storey and then progress further lower (Figure 5.11). The hinges are formed only in the beams along the web. That is, the beams along the direction of pushover loading are

developing plastic hinges. There is no formation of hinges in the flange of the building and the top 4-5 storeys in the web as well.

5.8.2 Mode 2 Pushover Analysis

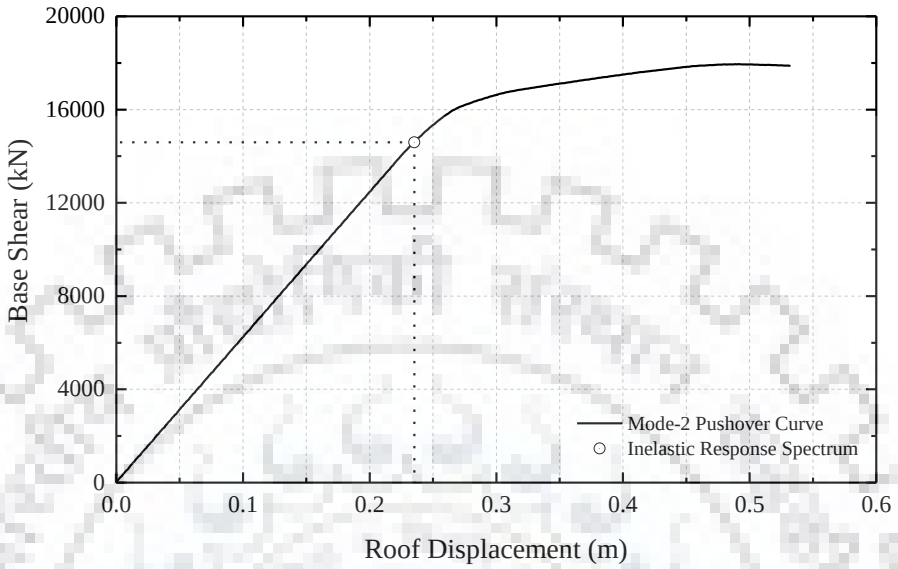

Figure 5.12 Mode 2 Pushover curve

The Pushover curve in the second mode after ignoring the post yield negative stiffness portion is shown in Figure 5.12. The corresponding peak deformation of inelastic SDOF system from inelastic response spectrum has been plotted as well.

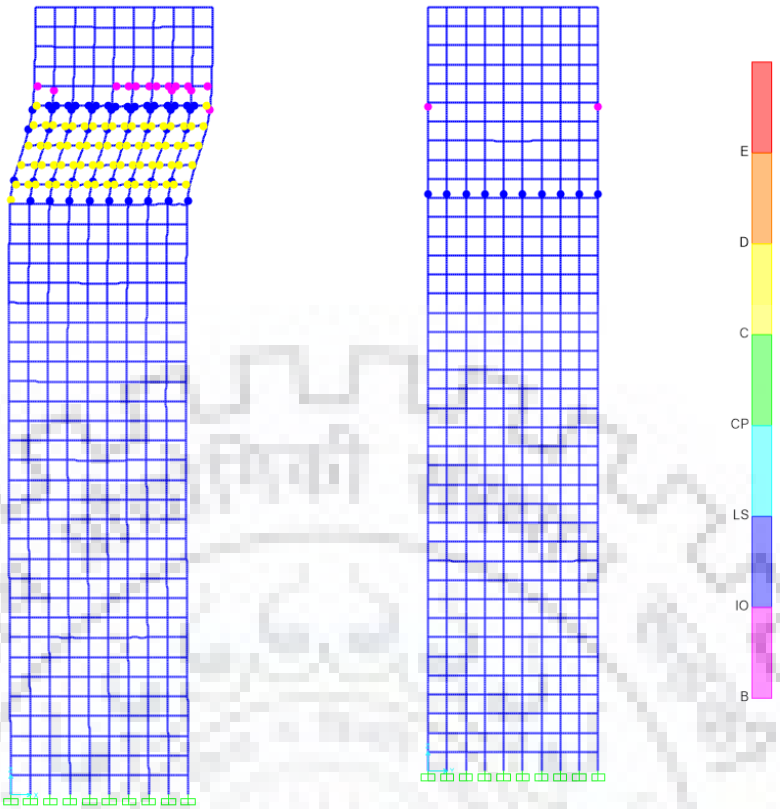

(a) (b)

Figure 5.13 Formation of hinges at the end of pushover analysis along Mode-2 in (a) X-Z plane (Web) and (b) Y-Z plane (Flange)

Pushover analysis in Mode -2 results in the plastic hinges forming only in the top 10 storeys and none in the bottom or intermediate storeys (Figure 5.13). This is due to the application of the pushover load proportional to the second mode shape. All the hinges are concentrated in the upper storeys, which is completely different from Mode-1 Pushover, wherein the hinge formation was concentrated to lower and intermediate storeys only.

5.8.3 Mode 3 Pushover Analysis

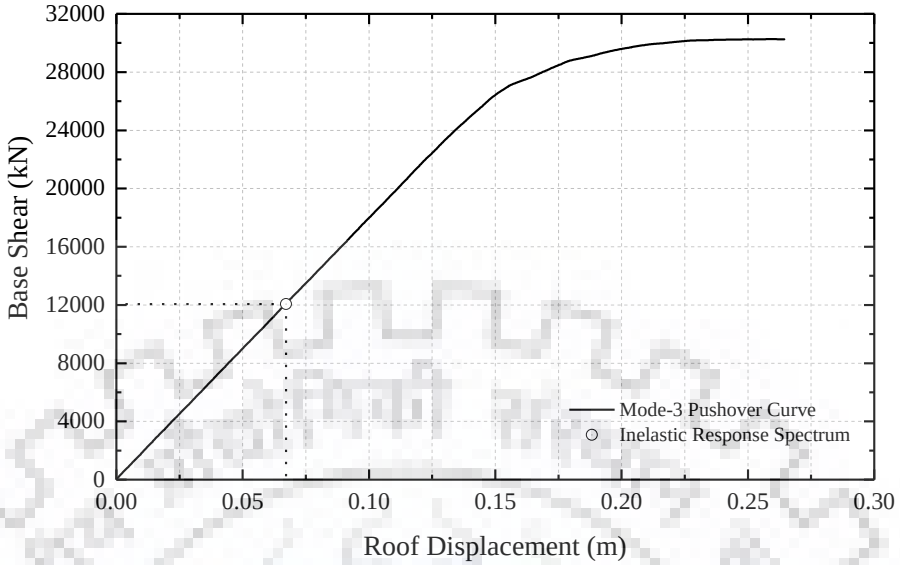

Figure 5.14 Mode 3 Pushover Curve

The Pushover curve in the third mode after ignoring the post yield negative stiffness portion is shown in Figure 5.14. The corresponding peak deformation of inelastic SDOF system from inelastic response spectrum has been plotted as well.

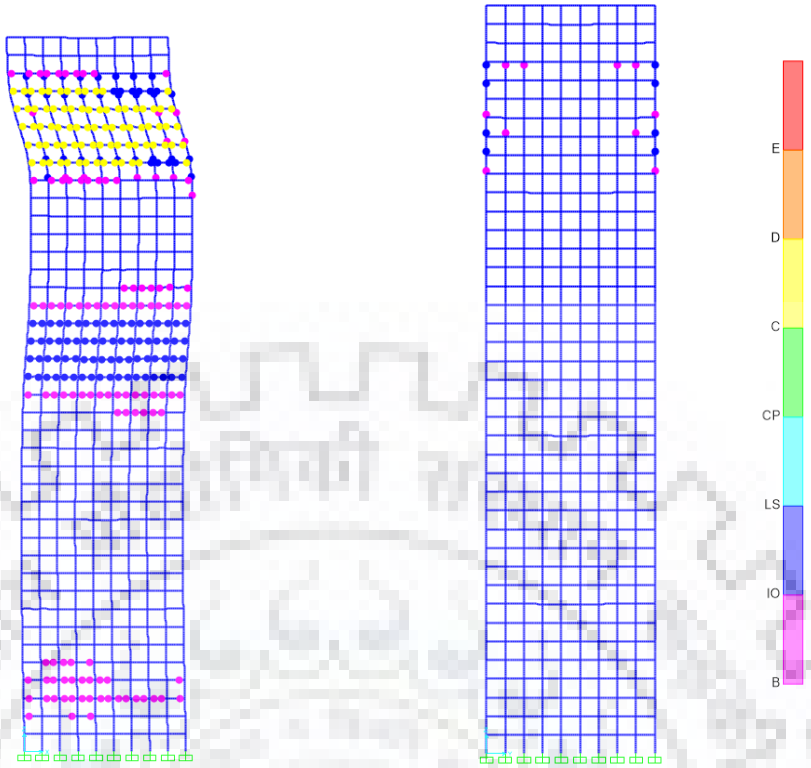

(a) (b)

Figure 5.15 Formation of hinges at the end of pushover analysis along Mode-3 in (a) X-Z plane (Web) and (b) Y-Z plane (Flange)

From Pushover Analysis along Mode-3, it can be observed that the formation of hinges is more at the top and intermediate storeys and less at the lower storeys (Figure 5.15).

From the above modal analysis, it can be seen that Mode-1 pushover shows the hinge formation in the lower storeys only and the formation of hinges at the top and intermediate storeys can be observed only for Mode-2 and Mode-3. This shows that the participation of the upper storeys is more when higher modes are considered. This can be more precisely understood when compared to the actual behaviour of the building under earthquake.

5.8.4 Shear Lag effect under Pushover loading

5.8.4.1 Without Gravity Loads

The Pushover analysis is carried out by considering load distribution along the height of the building proportional to the first mode of the building along that direction.

To get a more accurate behaviour of the effect of shear lag during pushover, the effect of gravity loads has been ignored. The variation of shear lag along the height for each modal pushover analysis under these conditions, is quite similar to the corresponding Modal shape of the structure.

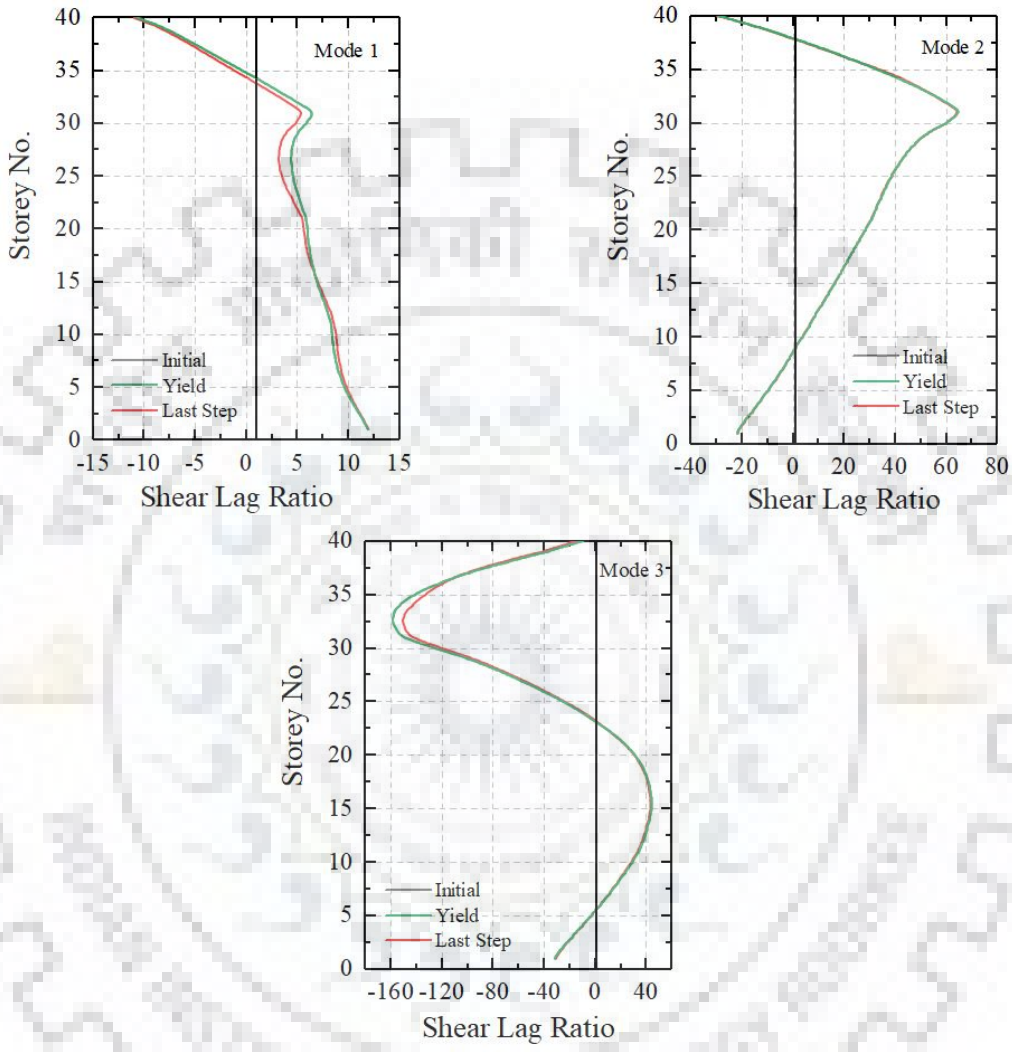

Figure 5.16 Variation of Shear lag ratio in the flange of the considered frame tube building, along the height, when subjected to pushover loading in Model-2

The shear lag variation along the height under pushover analysis for different modes is similar to its corresponding mode shapes. The shear lag variation during Pushover along Mode 1 is similar to that of lateral triangular load. This is as expected, because the loads are applied proportional to Mode 1, which is the same as a lateral triangular load along the height of the building.

From the above graphs, it can also be seen that the shear lag variation is same up until yield of structure, and is not affected much by nonlinearity during pushover analysis

ignoring the gravity loads. In Mode 1 and 3, slight decrease in shear lag towards the top can be observed, whereas in Mode -2, it is negligible.

5.8.4.2 With Gravity Loads

Considering the gravity loads, the pushover analysis yields the pushover or the capacity curve of the structure. The shear lag behaviour under this case also has been observed and studied.

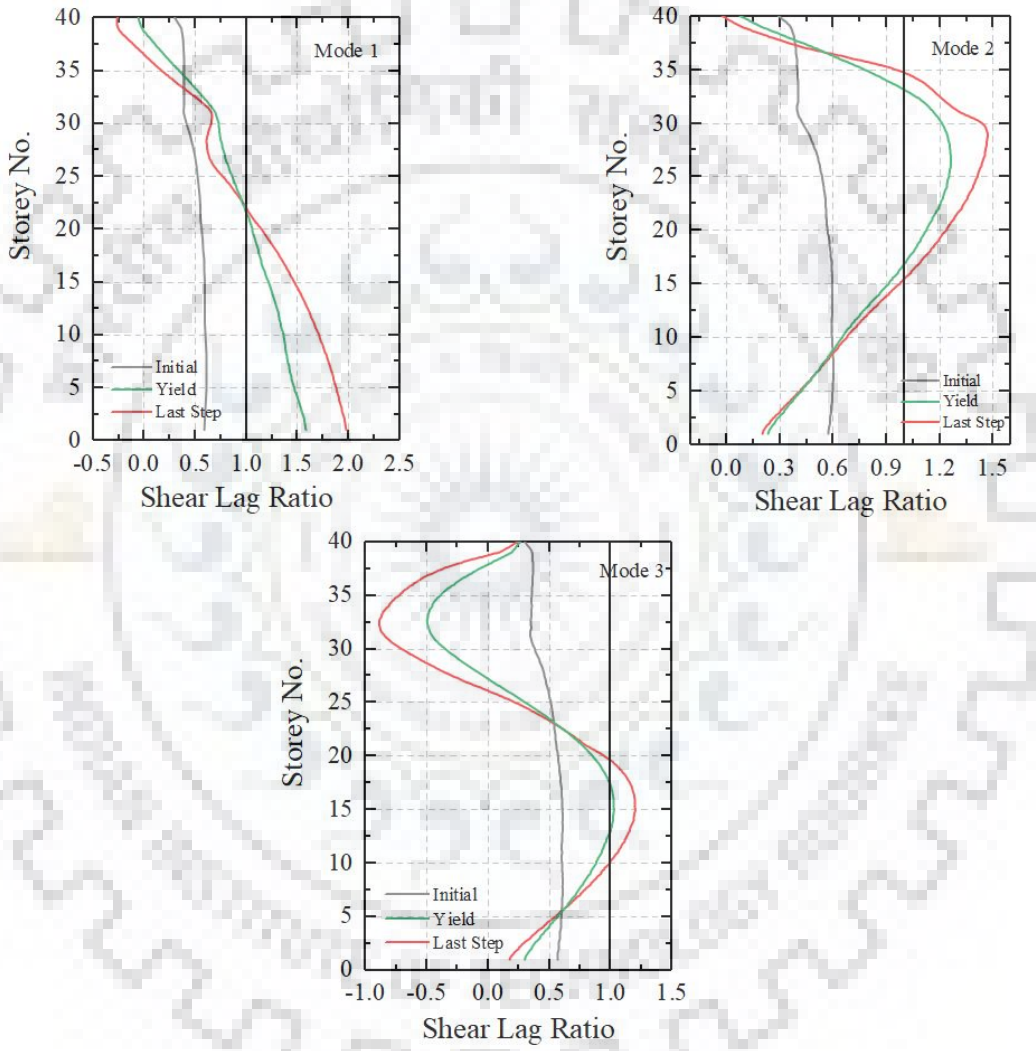

Figure 5.17 Variation of Shear lag ratio in the compression flange of the considered frame tube building, along the height, when subjected to pushover loading including gravity loads in Model-2

The Gravity loads, when considered has significantly reduced the shear lag effect in the compression flange columns. This is due to the triangular load distribution among the columns of the gravity loads, which causes a higher axial force in the centre columns than

the corner columns. Initially, the middle columns have almost twice the axial forces in the corner columns. But, as pushover progresses, this changes, with the positive shear lag at the bottom storeys and negative shear lag in the upper storeys for Mode-2. The point of shear lag reversal has shifted downwards in all the modes and their magnitude reduced significantly, when compared to the previous analysis excluding gravity loads. It is also noted that in Mode-2 and Mode-3, the shear lag increases only in the upper storeys or intermediate storeys and remains constant at the bottom storeys.

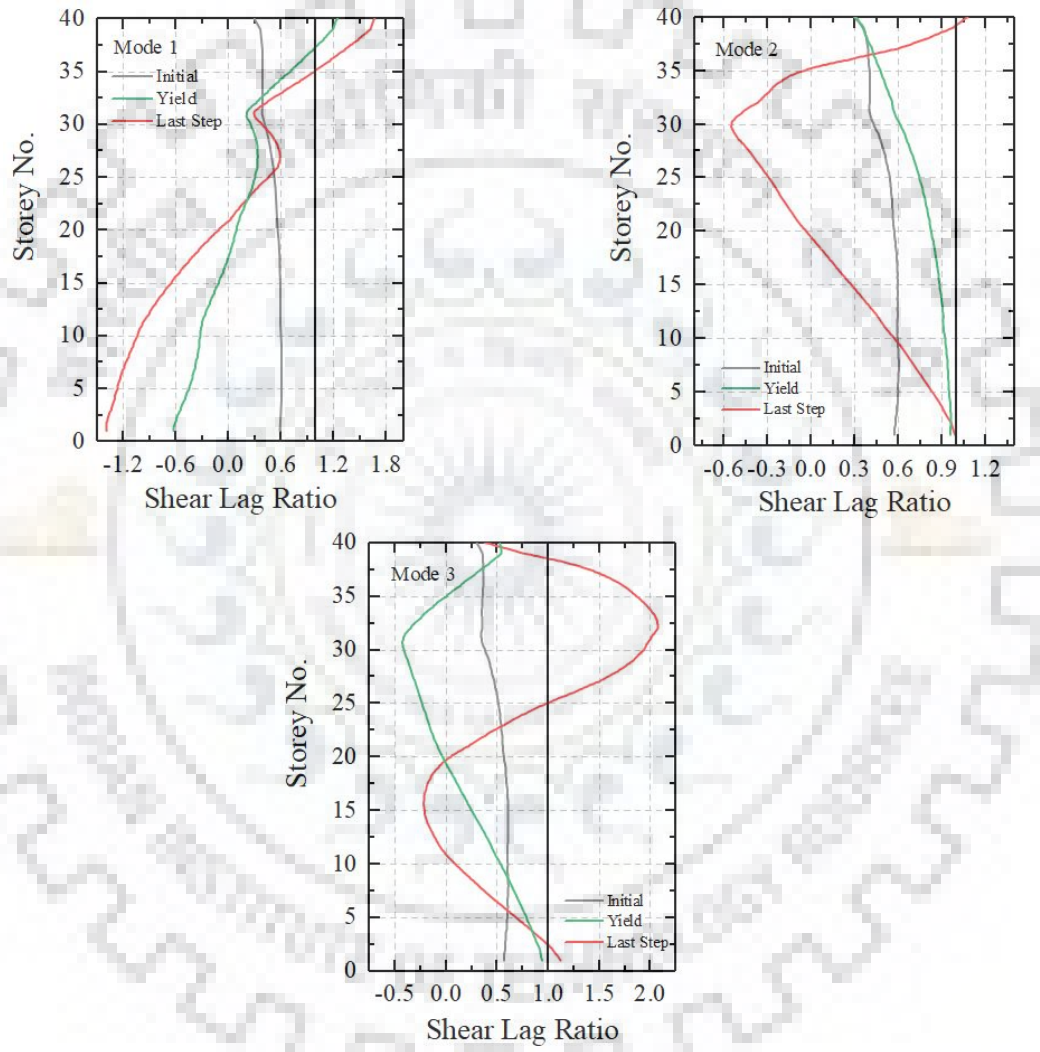

Figure 5.18 Variation of Shear lag ratio in the tension flange of the considered frame tube building, along the height, when subjected to pushover loading including gravity loads in Model-2

The Shear lag variation in the tension flange is quite different compared to the compression flange. The forces are opposite to that of the compressions side and hence, the shear lag variation also is a mirror image. In Mode-1, although it may seem like the

bottom storey columns are experiencing negative shear lag, in fact it implies that the gravity forces in the middle columns have not been overcome by the induced tensile forces due to pushover. The negative sign in this case indicates that the forces in the middle and corner columns are of opposite signs. The middle columns are in compression and the corner columns are in tension, hence, the shear lag ratio is resulting in negative. This implies that considering gravity masks the shear lag behaviour and hence cannot be accurately assessed.

5.9 Ground Motions

Far field ground motions were obtained from PEER database (https://ngawest2.berkeley.edu/) considering a fault distance of 10-50 km, shear wave velocity of 200m/s (Soil Type III) and a magnitude of 6-8. As per ASCE 7-16, a suite of 11 ground motions has been selected. Since, the structure being analysed is symmetric about both axes, the behaviour of the structure would be same irrespective of the direction of earthquake. The vertical ground motions have not been considered because of the absence of any type of vertical irregularities in the building.

The suite of 11 ground motions (Table 5.9) was selected after comparing their corresponding acceleration spectra with the target spectrum (IS Code Spectrum). Since, the structure is symmetric, time histories are considered for one direction, considering the maximum PGA. The comparison is carried out after suitable scaling of the ground motions specified in ASCE. In this study, amplitude scaling procedure has been adopted. The period ranges of interest taken is from 0.78s to 9.37s, which accounts for all the modes of the structure up to 90% modal mass participation.

Table 5.9 Selected Ground Motions

Record Sequence Number	Earthquake Name	Year	Station Name	Magnitude	PGA (g)	Mechanism	R_{jb} (km)	V_{s30} (m/sec)
162	"Imperial Valley-06"	1979	"Calexico Fire Station"	6.53	0.28	Strike slip	10.45	231.23
175	"Imperial Valley-06"	1979	"El Centro Array #12"	6.53	0.14	Strike slip	17.94	196.88
721	"Superstition Hills-02"	1987	"El Centro Imp. Co. Cent"	6.54	0.36	Strike slip	18.20	192.05
728	"Superstition Hills-02"	1987	"Westmorland Fire Sta"	6.54	0.17	Strike slip	13.03	193.67
757	"Loma Prieta"	1989	"Dumbarton Bridge West End FF"	6.93	0.13	Reverse Oblique	35.31	238.06
778	"Loma Prieta"	1989	"Hollister Differential Array"	6.93	0.27	Reverse Oblique	24.52	215.54
1203	"Chi-Chi_ Taiwan"	1999	"CHY036"	7.62	0.27	Reverse Oblique	16.04	233.14
5837	"El Mayor-Cucapah_ Mexico"	2010	"El Centro - Imperial & Ross"	7.20	0.38	Strike slip	19.39	229.25
5985	"El Mayor-Cucapah_ Mexico"	2010	"El Centro Differential Array"	7.20	0.55	Strike slip	22.83	202.26
6887	"Darfield_ New Zealand"	2010	"Christchurch Botanical Gardens"	7.00	0.16	Strike slip	18.05	187.00
6890	"Darfield_ New Zealand"	2010	"Christchurch Cashmere High School"	7.00	0.23	Strike slip	17.64	204.00

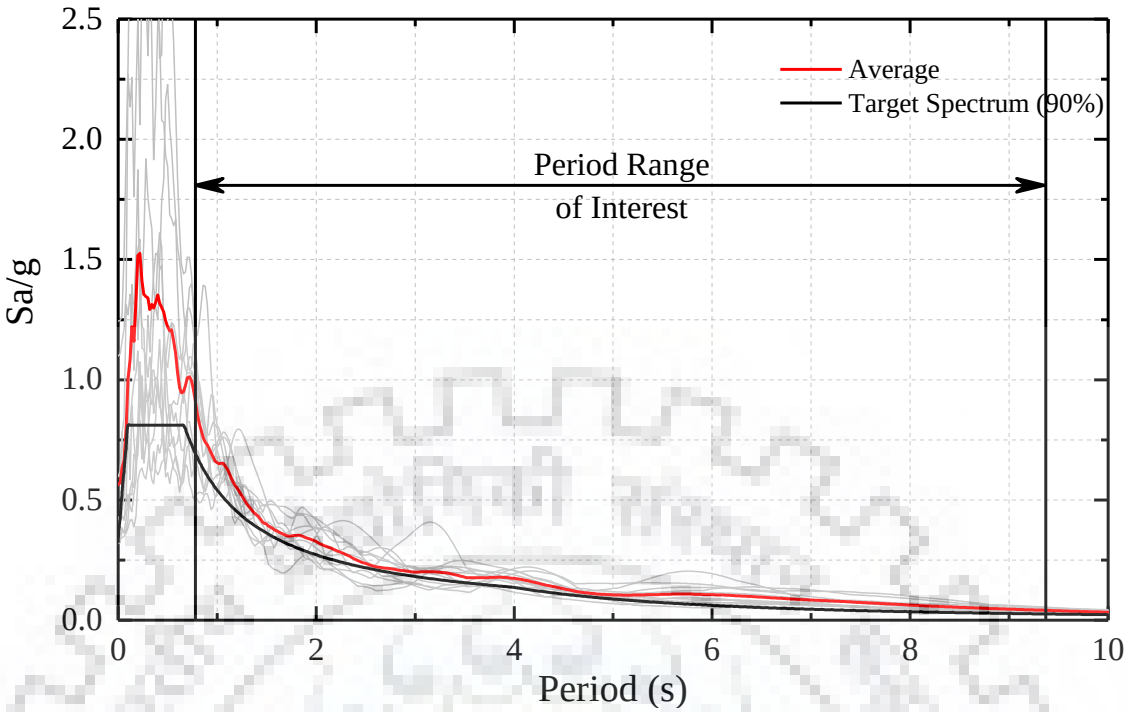

Figure 5.19 Average Response Spectrum of the ground motions

The Amplitude scaling method as in ASCE 7-16 recommends that the average of the acceleration spectrum of all 11 earthquakes should be greater than 0.9 times that of the target acceleration spectrum. The current target spectrum is the IS code spectrum for MCE (Maximum Credible Earthquake) for Zone V and soil type III given by IS 1893-2016. The ground motions were chosen carefully so that they meet this criterion in between the periods of interest of the building, as shown in Figure 5.19.

5.10 Time History Analysis

5.10.1 Damping

As mentioned previously, the damping in structures is usually assumed base on the type of structure (5% for RC and 2% for Steel). However, in high rise buildings, the damping is normally lower than traditionally assumed values. Based on new studies on existing buildings, it has been concluded that damping actually reduces with increasing height along the first translational mode, which is normally assumed on the higher side during conventional design (Smith et al., 2010).

IS 16700-2017 suggests damping ratio to not be greater than 2% for RC buildings. However, it does not specify the damping ratio to be taken for higher modes of the building.

Cruz and Miranda (2017) conducted a research study aimed at determining the actual damping ratio in tall buildings under real earthquakes. Their study was based on 14 instrumented tall buildings in California region. The modal damping ratio from these buildings were inferred from the acceleration recorded during real earthquakes. The buildings considered were ranging from 20-60 storeys and majorly consisted of moment frame type structural system.

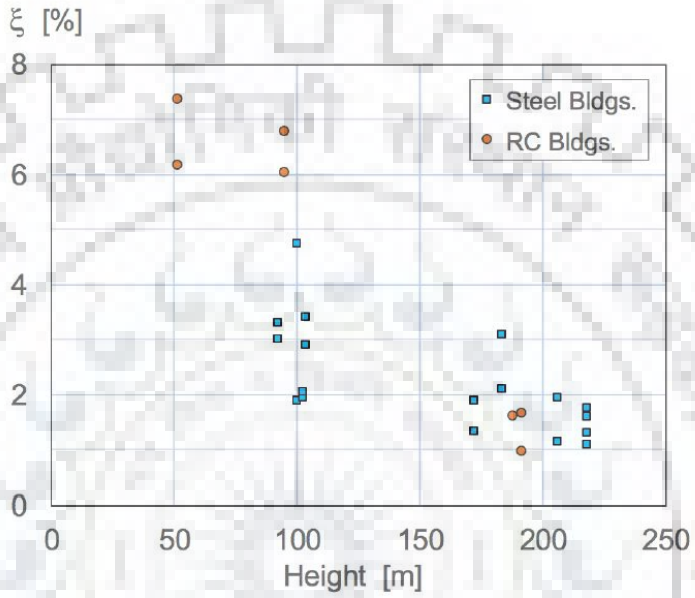

Figure 5.20 Damping ratios for the first translational mode of vibration (Cruz and Miranda, 2017).

They found that as per previous studies, damping ratio decreases with increase in height for the first translation mode and an empirical expression was given for its determination.

$$\xi = 3H^{-1} \tag{5.6}$$

Where, ξ - Damping ratio

H – the height of the building

The values obtained by their study were then compared with the 2.5% value recommendation by the Los Angeles Tall Buildings Structural Design Council (LATBSDC, 2011) and the 2% value recommended by the PEER Tall Building Initiative (PEER, 2009), which is the same as that recommended by IS code on Tall Building Design (IS 16700 - 2017). The codes have been found to overestimate the damping for buildings taller than 175m.

Further, they concluded that the damping ratio increases almost linearly for higher modes with increasing frequency and gave the following equation. This is supposedly due to inertial Soil structure interaction effects, wherein the radiation damping increases with increasing frequencies.

$$\xi_n = \xi_1 \times \left[1 + \gamma \left(\frac{f_n}{f_1} - 1 \right) \right] \tag{5.7}$$

where, γ - 0.11 for steel moment frame buildings, 0.13 for steel braced frame buildings and 0.12 for other buildings

f_n, f_1 and ξ_n, ξ_1 – the frequency of the n^{th} mode, the fundamental mode and their corresponding damping ratios.

Since the damping ratio of higher modes increases linearly, the Rayleigh Damping model is not preferred for Tall buildings. However, because of software limitations, the Rayleigh model has been used in the present study in for the damping ratios obtained from the above formulations, considering the first and the third mode of the building in each direction as shown in Table 5.10.

Table 5.10 Damping ratios for higher modes

Mode No.	**Period (s)**	**Frequency, *f* (Hz)**	**Damping ratio, ξ_n**
1	4.686	0.213	0.025
2	1.939	0.516	0.029
3	1.134	0.882	0.034

5.10.2 Hysteresis Parameters

The Hysteresis model used for the hinges in the current model is different for beams and columns. The Degrading Hysteresis model has been implemented for Beam M3 hinges. The degrading hysteresis parameters to be used were obtained from research papers.

Surana et al. (2018) obtained the hysteresis parameters required in SAP2000 by calibrating the analytical hysteretic model with the experimental results for nonconforming and conforming RC components according to IS13920. However, for column P-M2-M3 hinges, due to software limitations isotropic hysteresis model is used.

5.10.3 Base Shear

Table 5.11 Time History analysis base shears

Time History	Linear Analysis Base Shear (kN)		Non-linear Analysis Base Shear (kN)	
	Maximum	Minimum	Maximum	Minimum
TH162	50673.96	-48357.95	32741.94	-38914.60
TH175	43962.71	-49684.40	27638.08	-30942.10
TH721	31780.16	-39654.38	33980.61	-22245.45
TH728	43687.55	-46227.53	24950.91	-25944.46
TH757	47182.26	-52880.41	32801.56	-37899.68
TH778	35160.09	-45156.61	35737.14	-36917.43
TH1203	40488.73	-37750.63	28834.47	-27642.82
TH5837	33609.56	-40075.33	32551.35	-39747.26
TH5985	49797.46	-53717.66	30858.78	-30006.44
TH6887	36007.74	-34424.00	33226.60	-26064.59
TH6890	40796.58	-35984.02	27389.45	-31774.41
Average:	50673.96	-53717.66	35737.15	-39747.26

From Table 5.11, it can be seen that the base shears have reduced during non-linear analysis. This can be attributed to the fact that during non-linear analysis, the formation of hinges reduces the stiffness of the structure, hence attracting lesser force during the earthquake.

The base shear obtained from linear time history analysis can be compared to that obtained by other static and dynamic linear analysis by reducing these forces by the appropriate factors (Response reduction factor).

Hence, the average base shear from linear time history analysis for DBE after including importance factor of 1 and a response reduction factor of 5 is 5067.39 kN, which is slightly higher than that obtained by Response spectrum analysis (4274.68 kN), and almost equal to that obtained by static analysis (5112.73 kN). But, in non-linear analysis, the base shears obtained in comparison are much less than the one obtained by linear analysis, which can be considered accurate since it considers the actual behaviour of the building and its structural components as well.

5.10.4 Shear Lag

The Shear lag effect during time history analysis was studied at that instant of time when the roof displacement is maximum. For understanding the shear lag behaviour of the lateral loads only, the gravity loads have not been considered. Since the forces in the structural components reach their maximum value at different instants of time, it would not give an accurate assessment of shear lag in the structure. Hence, the shear lag behaviour is observed at that instant of time when the roof displacement is maximum.

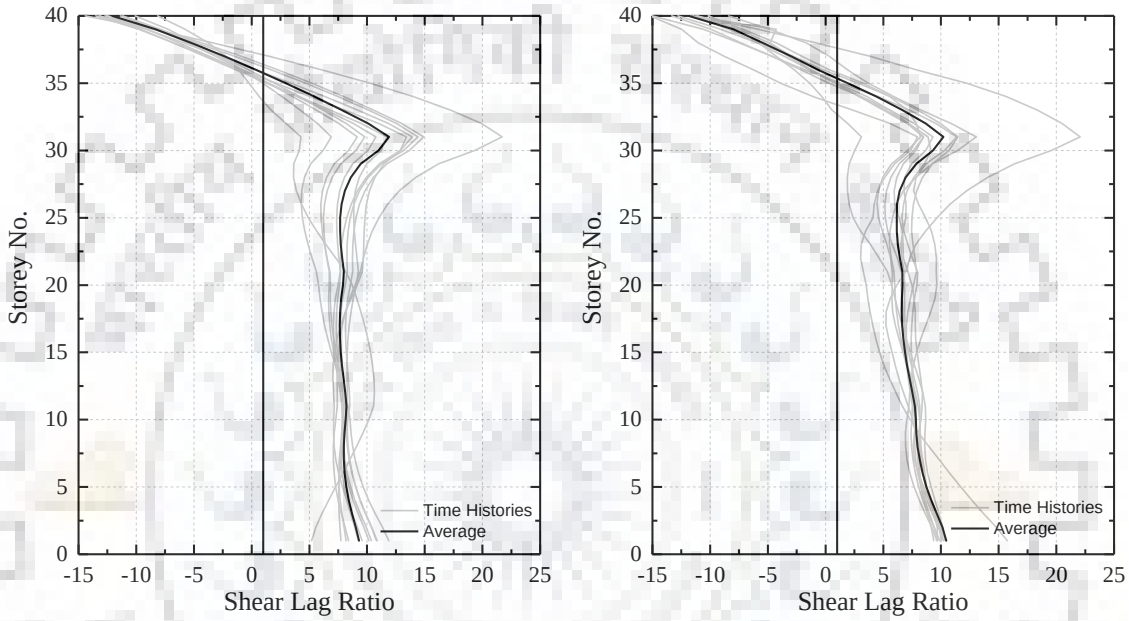

Figure 5.21 Variation of Shear lag ratio in the compression flange of the Model - 2, along the height, during (a) Linear and (b) Non-linear time history analysis

From Figure 5.21, it can be observed that the Shear lag in the structure flange is quite similar to the shear lag during lateral triangular load or constant acceleration. But, the positive shear lag at the bottom storeys are lower and are increasing up to certain height. The shear lag reversal in both linear as well as nonlinear case occurs at the 35th storey, slightly higher compared to lateral loads cases.

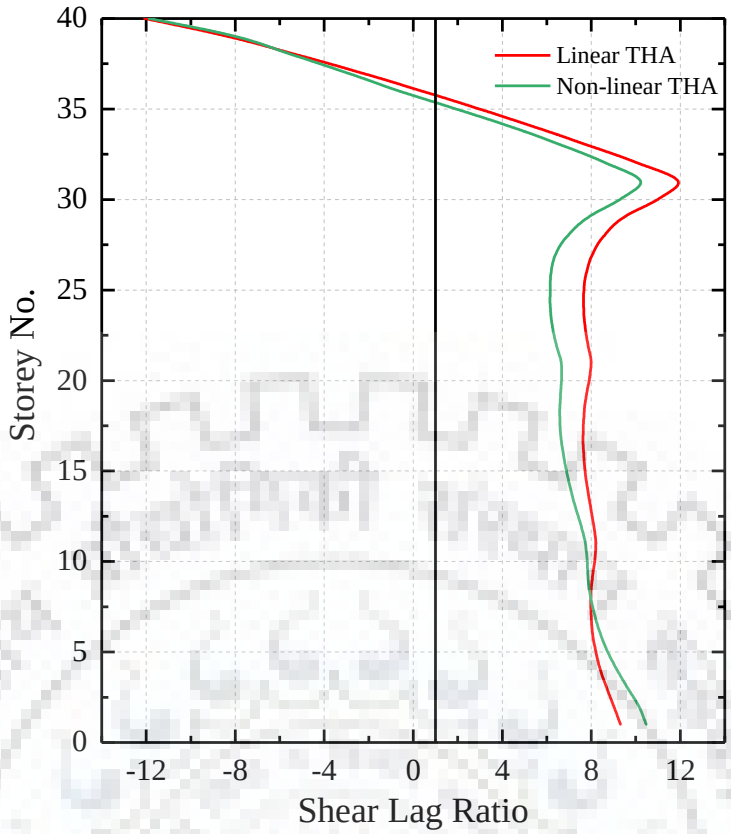

Figure 5.22 Comparison of Shear lag in linear and nonlinear time history analysis

In nonlinear time history analysis (NLTHA), the shear lag is slightly higher than in linear time history analysis (LTHA) up to the 8th storey, beyond which it is lower and keeps on decreasing and finally coincides with linear analysis after shear lag reversal at the 35th storey (Figure 5.22). This shows that the effect of non-linearity is quite insignificant as was the case during in Pushover analysis.

5.10.5 Hinge Formation Pattern

The hinge formation in the structure during nonlinear time history analysis (NLTHA) will give an accurate behaviour of the building during an earthquake. This is compared with the hinge formations during pushover analysis along different modes. The NLTHA is carried out in X-direction. Hence, the hinges are formed mainly in the web of the building, that is the direction parallel to the earthquake.

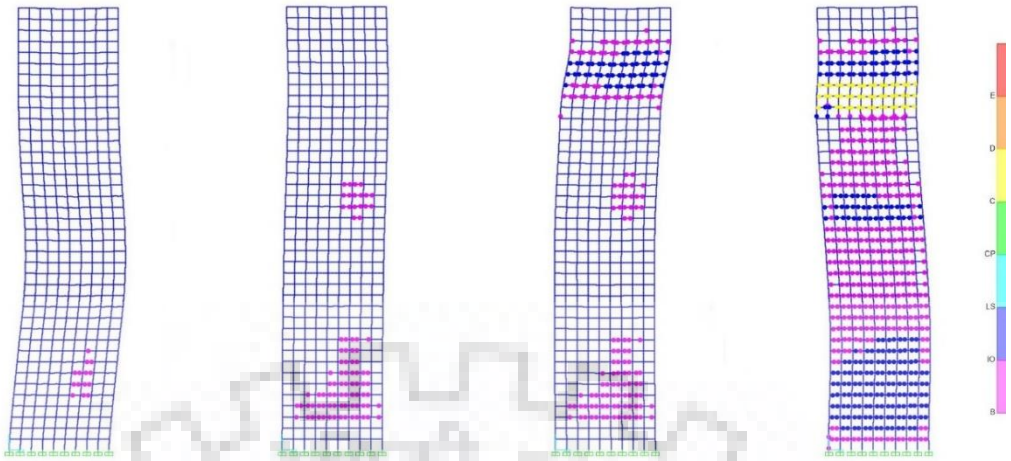

Figure 5.23 Stepwise hinge formation from start (left) to end (right) of time history along the web of the building during Non-linear Time History Analysis

Figure 5.23 shows the behaviour of the building and the hinge formation along the web of the building when subjected to a time history loading. The hinge formation pattern is quite similar in all 11 time histories, and only one of them has been shown above. It can be seen that the hinge formation starts at the bottom storey beams first and starts spreading. After a while, the hinges start forming in the upper storey beams as well and progresses throughout the building till the end of the time history as shown. At the end of time history, the hinges have formed in almost all the beams in the web of the building as shown in Figure 5.23.

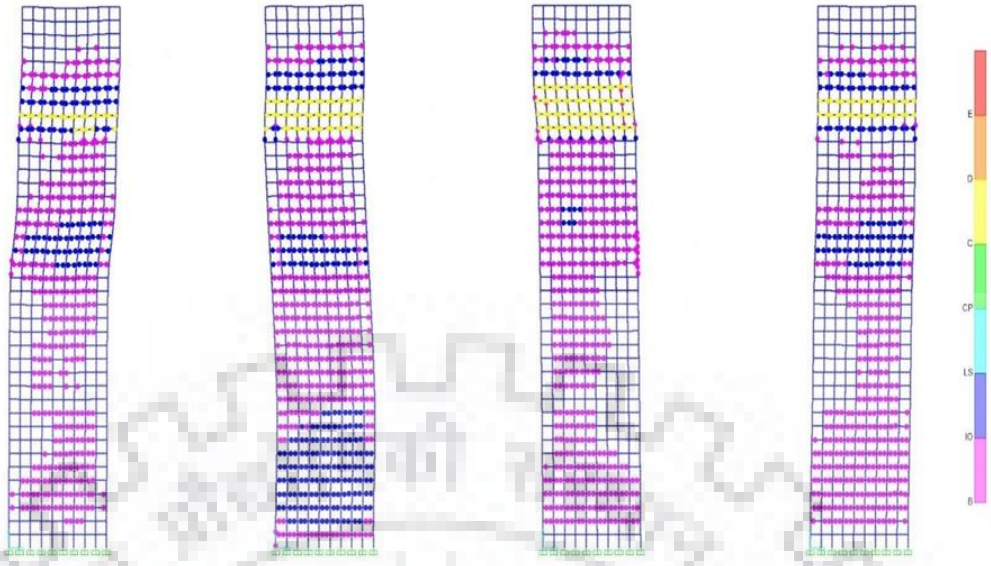

Figure 5.24 Hinge formation in web of the building for different ground motion histories.

It was observed that in most of the time history analysis, the hinge formation was similar, 4 of which are shown in Figure 5.24. The hinges are formed majorly in beams and a few in columns as well. The hinges are also spread throughout the building height and not restricted to lower storeys only. In Pushover analysis, along the 1st mode, the hinge formation in beams was more concentrated at the bottom and intermediate storeys only and pushover along the 2nd and the 3rd mode showed the formation of hinges in the upper storeys as well. Hence, it can be seen that the time history analysis results are a kind of combination of the hinges formed in the 3 modes of pushover analysis. That is, a single first mode pushover analysis is not able to completely capture the actual behaviour of the tall building subjected to lateral loads.

5.11 Roof Displacement and Inter-storey Drift

5.11.1 Linear Analysis

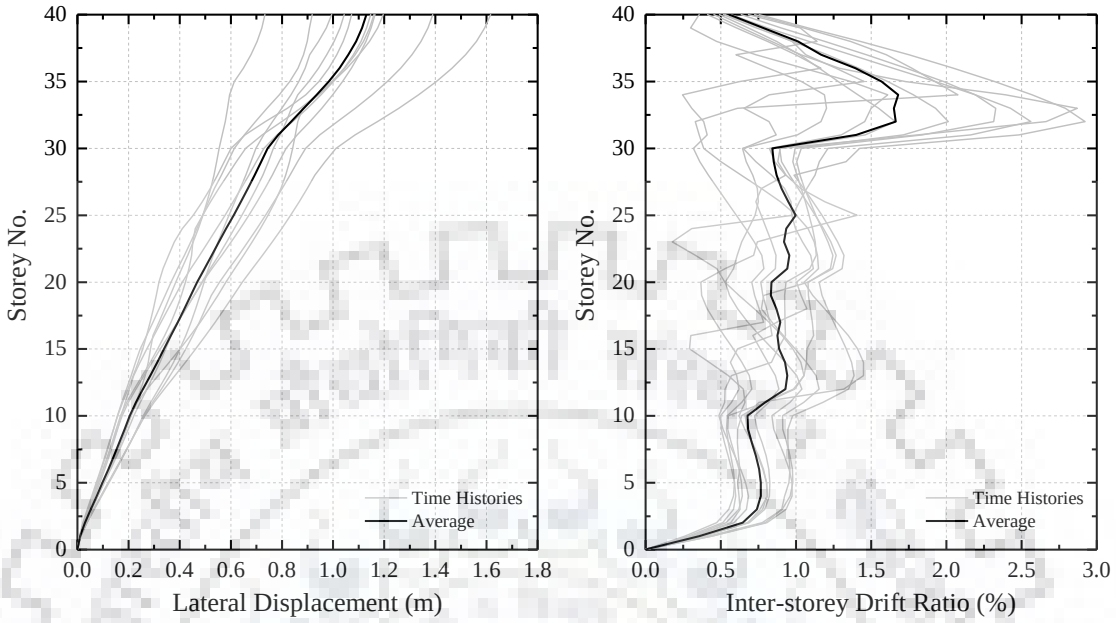

Figure 5.25 Linear Time history lateral displacements and inter-storey drift ratio

It can be seen from Figure 5.26 that the inter-storey drifts are higher in the upper storeys especially the top 10 storeys of the building. The linear time history results are now compared with results from other linear analyses, by modifying it with appropriate response reduction factor and zone factor.

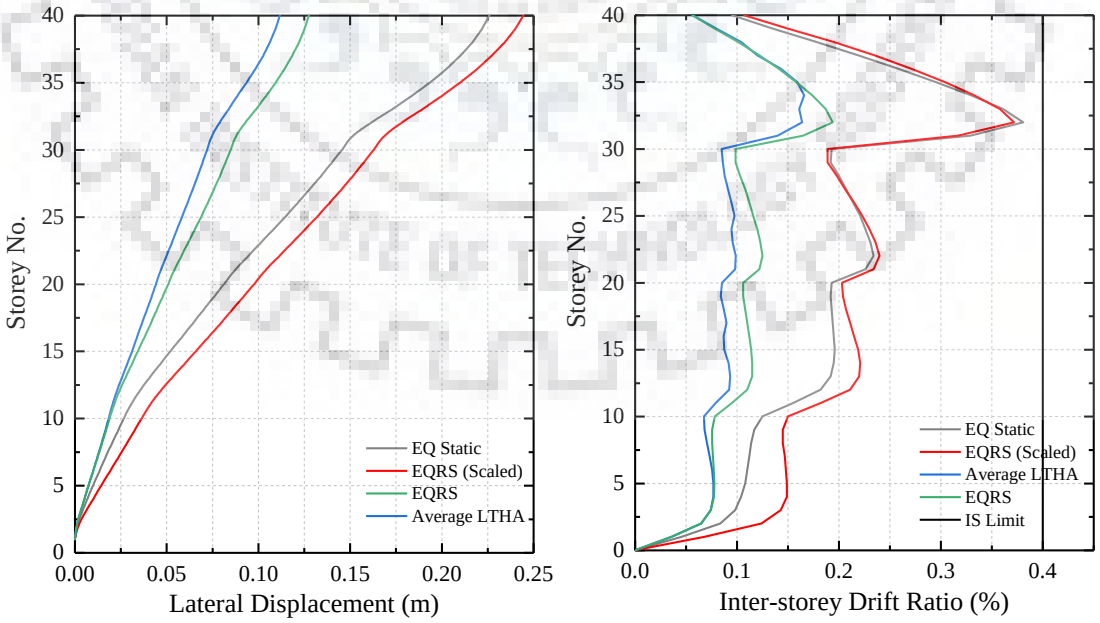

Figure 5.26 Lateral displacement and Inter-storey drift ratio of structure in different linear analyses

The lateral displacements obtained by linear time history and response spectrum analysis is less than that obtained by equivalent static analysis. The response spectrum analysis yields a much accurate results almost equal to that obtained by time history analysis, since it takes into consideration the contribution of higher modes as well. The equivalent static method gives much higher lateral displacements and is highly conservative. IS 16700-2017 recommends a maximum inter-storey drift ratio of 0.4% and the obtained results have been found to be well within the limits as shown in Figure 5.27.

5.11.2 Non-linear Analysis

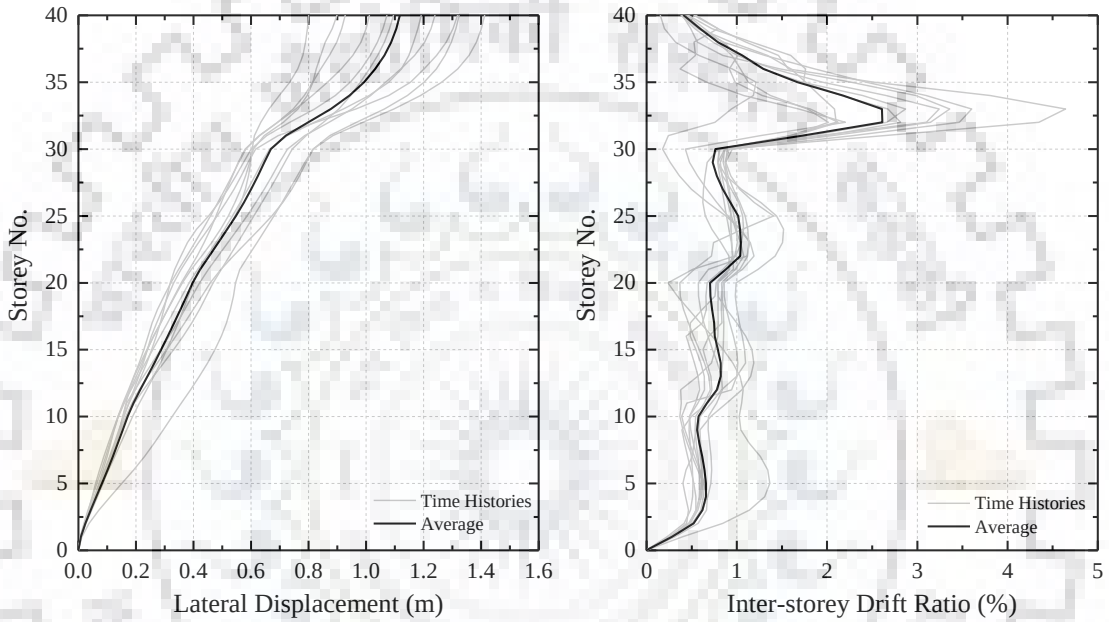

Figure 5.27 Non-linear Time History Analysis lateral displacement and inter-storey drift ratio

The nonlinear time history storey displacements of the building are slightly lower when compared to linear time history analysis. However, the inter-storey drift ratios are much higher in case of non-linear time history analysis, especially in the upper storeys. This is due to the non-linear hinges formed in the upper storey beams as shown in Figure 5.23. The NLTHA results are considered the exact response of the building and are used to compare with pushover analysis results.

The Pushover analysis carried out for each mode is combined by suitable appropriate methods, which is defined as the ‘Modal Pushover Analysis’. The pushover results when the lateral roof displacement is equal to the peak deformation of the inelastic SDOF system obtained from the inelastic response spectrum is extracted for each mode and combined by SRSS rule to obtain a more accurate response of the structure, considering

the effects of higher modes. This is compared with the NLTHA results as shown in Figure 5.28.

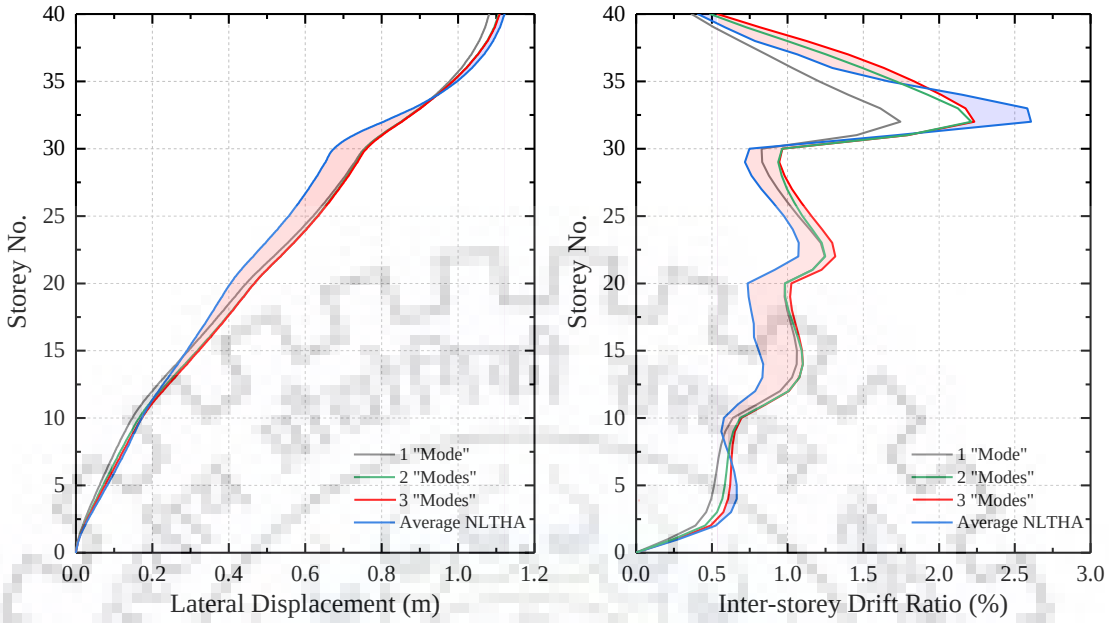

Figure 5.28 Lateral Storey displacements and Inter-storey drift ratios from MPA and NLTHA (average of all time histories); shading indicates errors in MPA including SRSS of three ‘modes’.

It is observed that the MPA procedure gives reasonably accurate results. It can be seen that considering more than one mode does not result in much difference for storey displacements. However, the inclusion of just the second mode only results in significant improvement in the inter-storey drifts (especially the upper storeys) and inclusion of the third mode as well does not affect the results to a great extent.

The lateral storey displacements are accurate for lower storeys, is on the higher side for intermediate storeys and slightly lower for upper storeys. The Inter-storey drifts obtained by MPA is underestimated in lower storeys, overestimated in middle storeys and slightly varying about the NLTHA values in the upper storeys, as shown in Figure 5.27.

CHAPTER 6: CONCLUSIONS

In the current study, a 40-storey building was designed as per relevant Indian codes and then subjected to various loads to study its performance. The building was subjected to different types of lateral loads including UDL, triangular load, point load and a constant acceleration. Nonlinear static and dynamic analyses were also performed on the building and compared with the corresponding linear analyses.

From the results of the analyses, the shear lag in the structure was studied and the following conclusion have been drawn-

- The Shear lag effect in tall buildings are dependent on the stiffness of the columns as well as the stiffness of the interconnecting beams. Shear lag can be significantly reduced by making the interconnecting beams more rigid. However, it could not be completely eliminated.
- The shear lag magnitude and its reversal depend on the structural parameters of the building and their variation along the height like the beam and column sizes, type of loading, number of storeys and number of bays.
- A framed tube structure with uniform properties along the height has a lower magnitude of shear lag ratio than a structure with gradually varying properties along the height (decreasing sizes with increase in height) for the same type of lateral loading. Consequently, the shear lag reversal occurs at a lower storey for a structure with uniform properties in comparison with a structure with varying properties.
- The variation of shear lag ratio in different modes of the building is similar to its corresponding mode shapes. The shear lag variation was found to be unaffected by material and structural nonlinearity. Although there is a change in the shear lag ratio, the increase or decrease in its magnitude is small.
- The shear lag ratio under gravity loads is opposite to that of lateral loads, with higher axial force in the centre columns and lower axial forces in the corner columns. When gravity loads were combined with pushover loading, the shear lag ratio was found to decrease and the level of shear lag reversal shifts downwards, as pushover progresses. This is contrary to the observation in case of pushover under lateral load alone, where the level of reversal of shear lag shifts upward with progress of pushover (i.e. under increasing inelasticity).

- The shear lag effect during time history analysis without considering the gravity loads showed that the variation is quite different compared to that under other lateral load variations. The earthquake loading shows increasing shear lag with increase in height, which was not the case for other types of loading. This might be the result of the higher mode effects, which are not considered in static loadings. From Mode-2 and Mode-3 pushover analysis, it can be seen that the shear lag is quite high at around the top storey, which can also be observed in time history. But, the variation at the lower storeys is similar to that of Mode-1 pushover. And, the nonlinearity in time history increased the shear lag at the bottom storeys only and decreased the shear lag at the intermediate and upper storeys. The effect of nonlinearity on shear lag is small, as in case of pushover analysis.

The behaviour of the structure was studied through nonlinear analysis. The effects of higher modes of the building in its behaviour was compared and the following conclusion have been made-

- The linear static analysis estimates the forces and response considering the first mode only and ignores the contribution of the higher modes. Hence, it was found that this overestimates the actual response of the building, resulting in higher base shears and inter-storey drifts than the actual. More accurate response was obtained by a linear dynamic analysis (Response Spectrum Method/Time History Analysis) when compared with the linear static analysis.
- The nonlinear static analysis, using load distribution proportional to the fundamental mode, was found to be unable to fully capture the actual behaviour of the structure as obtained using a nonlinear dynamic analysis (Nonlinear Time History Analysis). The Mode-1 pushover analysis yields the storey displacements and inter-storey drifts in close agreement with the nonlinear time history analysis results at the lower storeys only and underestimates the response in the upper storeys.
- The response of the structure obtained from the pushover analysis considering different modes was combined using the 'Modal Pushover Analysis' procedure. This method was found to underestimate the floor displacements and the inter-storey drifts in lower storeys, and to overestimate them in the

intermediate storeys. In the upper storeys, even though the floor displacements were coinciding with the nonlinear analysis results, the corresponding inter-storey drifts were not matching.

- The first mode pushover analysis resulted in the formation of beam plastic hinges in the lower and intermediate storeys only, while the second and third mode resulted in hinge formation in various upper storey levels as well. On the other hand, the nonlinear time history analysis resulted in a significant number of hinges in the upper storey beams. This is a clear indication of the influence the higher modes have on the behaviour of a tall building during an earthquake.
- The plots of lateral storey displacements, inter-storey drifts, and the plastic hinge patterns indicate that the inclusion of second mode significantly improves the accuracy of the results, whereas inclusion of the third mode has only marginal changes in the response. However, as reported by Chopra and Goel (2002) the MPA procedure produces large errors (up to 100%) in plastic hinge rotations. Hence, the MPA procedure is applicable for calculating the storey displacements and the inter-storey drifts only.

REFERENCES

1. Ali, M. M., and Moon, K. S. (2007). "Structural Developments in Tall Buildings: Current Trends and Future Prospects." *Architectural Science Review*, 50(3), 205-223.
2. Applied Technology Council. (1996). "Seismic Evaluation and Retrofit of Concrete Buildings." *ATC-40*, Redwood City, California.
3. ASCE. (2016). "Minimum Design Loads and Associated Criteria for Buildings and Other Structures." *ASCE/SEI 7*, Reston, Virginia.
4. ASCE. (2017). "Seismic Evaluation and Retrofit of Existing Structures." *ASCE/SEI 41*, Reston, Virginia.
5. BIS (Bureau of Indian Standards). (1987). "Code of Practice for Design Loads (other than Earthquake) for Buildings and Structures - Dead Loads." *IS 875 (Part 1)*, New Delhi, India.
6. BIS (Bureau of Indian Standards). (1987). "Code of Practice for Design Loads (other than Earthquake) for Buildings and Structures - Imposed Loads." *IS 875 (Part 2)*, New Delhi, India.
7. BIS (Bureau of Indian Standards). (2000). "Plain and Reinforced Concrete – Code of Practice." *IS 456*, New Delhi, India.
8. BIS (Bureau of Indian Standards). (2016). "Criteria of Earthquake Resistant Design of Structures: General Provisions and Buildings." *IS 1893-Part 1*, New Delhi, India.
9. BIS (Bureau of Indian Standards). (2017). "Criteria for Structural Safety of Tall Concrete Buildings." *IS 16700*, New Delhi, India.
10. Chopra, A. K., and Goel, R. K. (2002). "A modal pushover analysis procedure for estimating seismic demands for buildings." *Earthquake Engineering & Structural Dynamics*, 31(3), 561-582.
11. Connor, J. J., and Pouangare, C. C. (1991). "Simple Model for Design of Framed-Tube Structures." *Journal of Structural Engineering*, 117(12), 3623-3644.
12. Cruz, C., and Miranda, E. (2017). "Evaluation of Damping Ratios for the Seismic Analysis of Tall Buildings." *Journal of Structural Engineering*, 143(1), 04016144.

13. De Stefano, M., Nudo, R., and Viti, S. (2004). "Evaluation of Second Order effects on the Seismic Performance of RC Framed Structures: A Fragility Analysis." *13th World Conference on Earthquake Engineering* Vancouver, B. C., Canada, 428.
14. European Committee for Standardization. (2004). "Design of structures for earthquake resistance – Part 1: General rules, seismic actions and rules for buildings." *EN 1998-1/Eurocode 8*, Rue de Stassart, Brussels.
15. FEMA. (2000). "Prestandard and Commentary for the Seismic Rehabilitation of Buildings." *FEMA 356*, Washington, DC.
16. Fintel, M. (1974). *Handbook of Concrete Engineering*, Van Nostrand Reinhold Company Inc., New York.
17. Gaur, H., and Goliya, K. R. (2015). "Correlating Stiffness and Shear Lag Behavior with Brace Configuration of Tall Truss Tube Buildings." *Buildings*, 5(3).
18. Inel, M., and Ozmen, H. B. (2006). "Effects of plastic hinge properties in nonlinear analysis of reinforced concrete buildings." *Engineering Structures*, 28(11), 1494-1502.
19. Křístek, V., and Bauer, K. (1993). "Stress Distribution in Front Columns of High-Rise Buildings." *Journal of Structural Engineering*, 119(5), 1464-1483.
20. LATBSDC (Los Angeles Tall Buildings Structural Design Council). (2011). "An alternative procedure for seismic analysis and design of tall buildings located in the Los Angeles region." Los Angeles, CA.
21. Lee, K.-K., Loo, Y.-C., and Guan, H. (2001). "Simple Analysis of Framed-Tube Structures with Multiple Internal Tubes." *Journal of Structural Engineering*, 127(4), 450-460.
22. Mazinani, I., Jumaat, M. Z., Ismail, Z., and Chao, O. Z. (2014). "Comparison of shear lag in structural steel building with framed tube and braced tube." *Structural Engineering and Mechanics*, 49.
23. *OriginPro 2017* [Computer software]. OriginLab Corporation, Northampton, MA.
24. Park, R., and Paulay, T. (1975). *Reinforced concrete structures*, John Wiley & Sons Inc.
25. PEER (Pacific Earthquake Engineering Research Centre) (2009). "Guidelines for Performance-Based Seismic Design of Tall Buildings." Berkeley, CA.

26. PEER (Pacific Earthquake Engineering Research Centre). 2011. "PEER ground-motion database." (https://ngawest2.berkeley.edu/site).
27. *SAP2000 Ultimate version 20.0.0* [Computer software]. Computer and Structures, Inc., Berkeley, CA.
28. Shinde, A. (2017). "Dynamic Analysis of RC Framed Tube Structures." *Dynamic Analysis of RC Framed Tube Structures*, 4(5), 2368-2373.
29. Shushkewich Kenneth, W. (1991). "Negative Shear Lag Explained." *Journal of Structural Engineering*, 117(11), 3543-3546.
30. Singh, Y., and Nagpal, A. K. (1994). "Negative Shear Lag in Framed-Tube Buildings." *Journal of Structural Engineering*, 120(11), 3105-3121.
31. Smith, R., Merello, R., and Willford, M. (2010). "Intrinsic and supplementary damping in tall buildings." *Proceedings of the Institution of Civil Engineers - Structures and Buildings*, 163(2), 111-118.
32. Surana, M., Singh, Y., and Lang Dominik, H. (2018). "Seismic Characterization and Vulnerability of Building Stock in Hilly Regions." *Natural Hazards Review*, 19(1), 04017024.